2020 1st Season Stock Assessment

Falkland calamari

(*Doryteuthis gahi*)

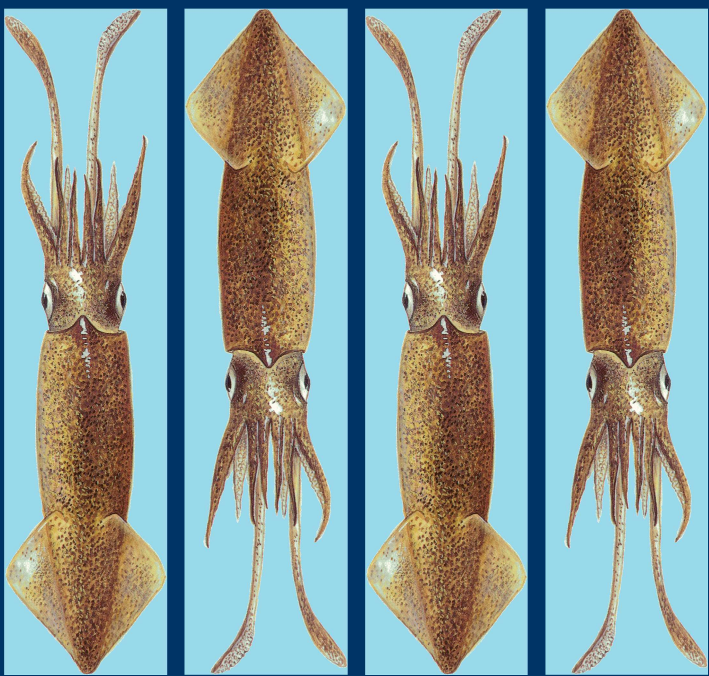

S1 - 2020 - LOL

Andreas Winter

Natural Resources - Fisheries
Falkland Islands Government
Stanley, Falkland Islands

July 2020

Index

Summary

1) The 2020 first season *Doryteuthis gahi* fishery (C license) was open from February 24th, and closed by directed order on April 28th. Compensatory days for mechanical problems and bad weather resulted in 20 vessel-days taken after April 28th, with one vessel fishing as late as May 1st.
2) Four fishing mortalities of Southern sea lions and one fishing mortality of South American fur seal were recorded throughout the course of the season. The use of Seal Exclusion Devices was mandated north of 52° 15' S starting on March 6th, and mandated south of 52° 15' S starting on March 18th.
3) 29,116 tonnes of *D. gahi* catch were reported in the 2020 C-license fishery; the lowest first season catch since 2016 and giving an average CPUE of 28.8 t vessel-day^{-1}. During the season 74.9% of *D. gahi* catch and 72.2% of fishing effort were taken south of 52° S; 25.1% of *D. gahi* catch and 27.8% of fishing effort were taken north of 52° S.
4) In the south sub-area, six depletion periods / immigrations were inferred to have started on February 24th (start of the season), March 3rd, March 9th, April 7th, April 15th, and April 27th. In the north sub-area, 5 depletion periods / immigrations were inferred to have started on February 28th (start of fishing), March 3rd, April 2nd, April 12th, and April 16th.
5) Approximately 24,947 tonnes of *D. gahi* (95% confidence interval: 22,717 to 42,625 t) were estimated to have immigrated into the Loligo Box after the start of first season 2020, of which 19,698 t south of 52° S and 5,249 t north of 52° S.

   The escapement biomass estimate for *D. gahi* remaining in the Loligo Box at the end of first season 2020 was: Maximum likelihood of 19,822 tonnes, with a 95% confidence interval of 15,233 to 37,088 tonnes.

   The risk of *D. gahi* escapement biomass at the end of the season being less than 10,000 tonnes was estimated at effectively zero.

Introduction

The first season of the 2020 *Doryteuthis gahi* fishery (Patagonian longfin squid – colloquially *Loligo*) opened on February 24th. One vessel delayed entry by 3 days for repairs and upgrade. Two other vessels took a combined 4 flex days (FIFD / LPG 2017) for mechanical repairs, and one of these vessels transferred days to a partner vessel. Fifteen flex days were taken for in-season bad weather, of which fourteen on April 22nd (Figure 1). The season ended by directed closure on April 28th, and the various schedule flex adjustments amounted to 22 vessel-days deferred after April 28th. However, one vessel waived its last two days of deferred fishing rather tranship and return for a single remaining day, resulting in May 1st as the final date of the fishing season.

As in previous seasons, all C-license vessels were required to embark an observer tasked (at minimum) to monitor the presence and incidental capture of pinnipeds (Iriarte et al. 2020). The occurrence of pinniped mortalities resulted in mandatory use of Seal Exclusion Devices (SEDs) north of 52° 15' S starting on March 6th, and south of 52° 15' S starting on March 18th. Similar to first season 2019 (Winter 2019a), fishing was closed early north of 52°S (on April 23rd; decision on April 20th) because of small sizes of the squid (Figure 2).

Total reported *D. gahi* catch under first season C license was 7,312 north + 21,804 south = 29,116 tonnes (Table 1), corresponding to an average CPUE of 29116 / 1012 = 28.8 tonnes vessel-day^{-1}. Both catch and average CPUE were the lowest for a first season since 2016, but catch was above median for the first season time series since 2004, and average CPUE was exactly the median (Table 1).

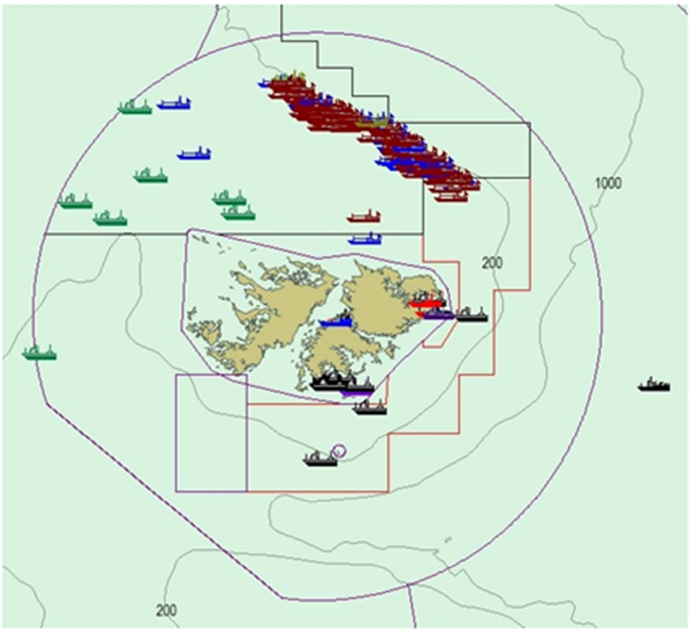

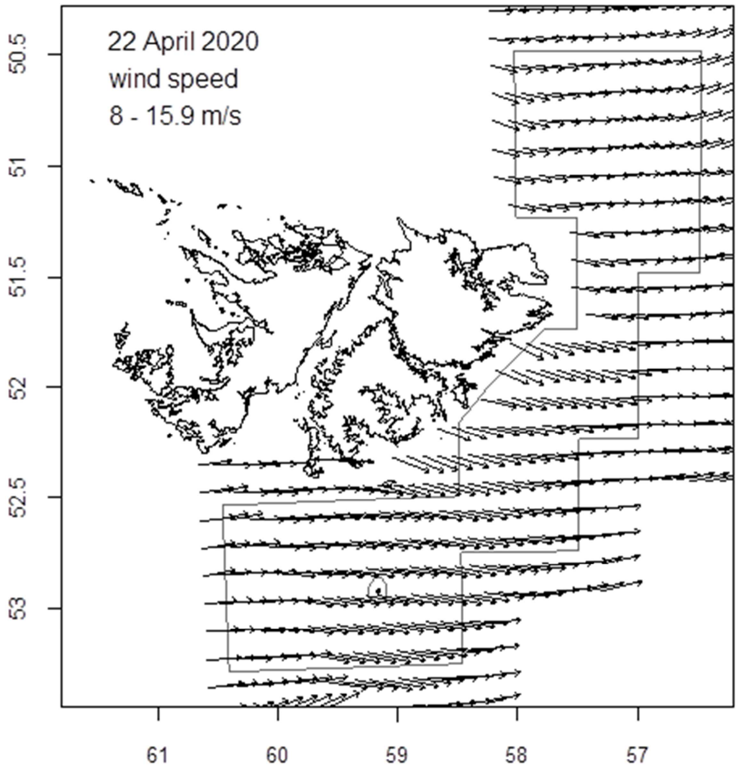

Figure 1. Fish Ops chart display and wind speed vector plot (Copernicus Marine Service) on April 22nd, when only two C-licensed vessels fished.

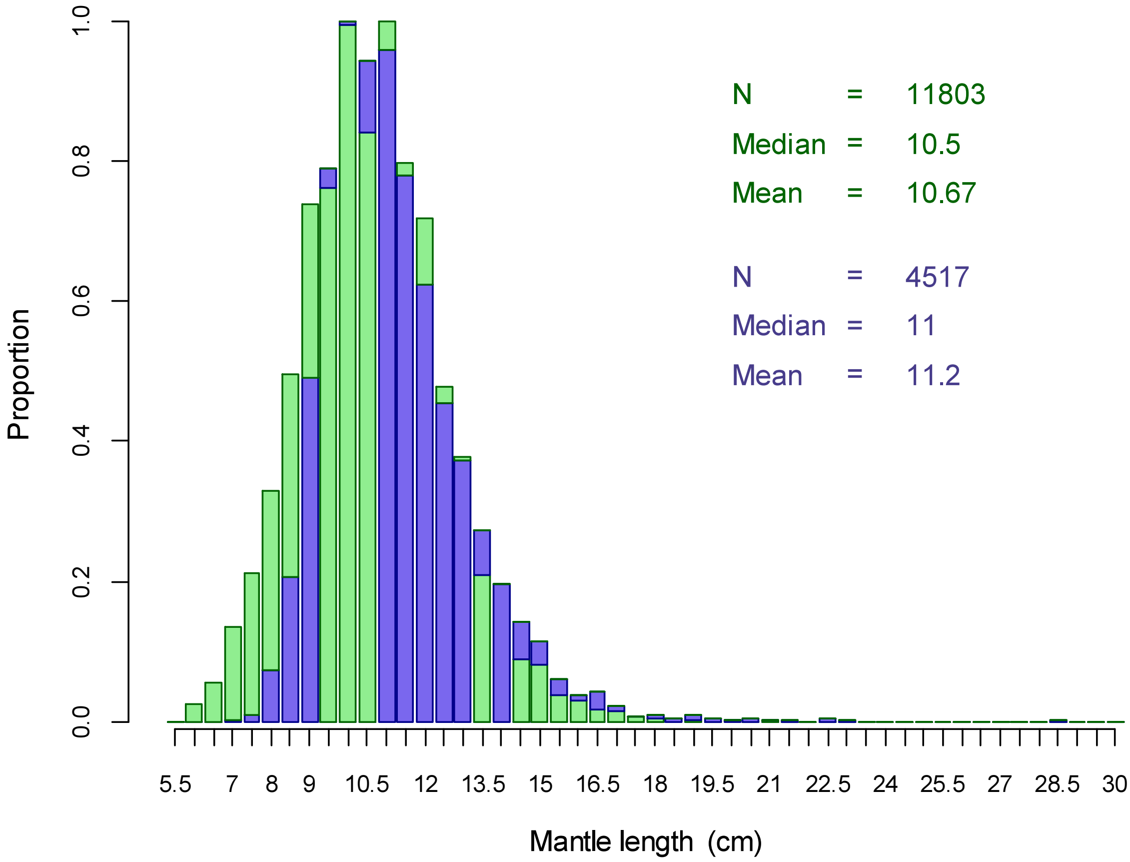

Figure 2 [previous page]. *D. gahi* observer length-frequency distributions from April 13th to April 22nd 2020, the ten days up to closure of the north sub-area. In the north (green) 23.0% of individuals had mantle lengths ≤ 9 cm. In the south (purple) 10.2% of individuals had mantle lengths ≤ 9 cm.

Assessment of the Falkland Islands *D. gahi* stock was conducted with depletion time-series models as in previous seasons (Agnew et al. 1998, Roa-Ureta and Arkhipkin 2007; Arkhipkin et al. 2008), and in other squid fisheries (cited in Arkhipkin et al. 2020). Because *D. gahi* has an annual life cycle (Patterson 1988, Arkhipkin 1993), stock cannot be derived from a standing biomass carried over from prior years (Rosenberg et al. 1990, Pierce and Guerra 1994). The depletion model instead calculates an estimate of population abundance over time by evaluating what levels of abundance and catchability must be present to sustain the observed rate of catch. Depletion modelling of the *D. gahi* target fishery is used both in-season and for the post-season summary, with the objective of maintaining an escapement biomass of 10,000 tonnes *D. gahi* at the end of each season as a conservation threshold (Agnew et al. 2002, Barton 2002).

Table 1. *D. gahi* season comparisons since 2004, when catch management was assumed by the FIFD. Days: total number of calendar days open to licensed *D. gahi* fishing including (since 1st season 2013) optional extension days; V-Days: aggregate number of licensed *D. gahi* fishing days reported by all vessels for the season. Entries in italics are seasons closed by emergency order.

	Season 1			Season 2		
	Catch (t)	Days	V-Days	Catch (t)	Days	V-Days
2004	7,152	46	625	17,559	78	1271
2005	24,605	45	576	29,659	78	1210
2006	19,056	50	704	*23,238*	*53*	*883*
2007	17,229	50	680	*24,171*	*63*	*1063*
2008	24,752	51	780	26,996	78	1189
2009	12,764	50	773	*17,836*	*59*	*923*
2010	28,754	50	765	36,993	78	1169
2011	15,271	50	771	*18,725*	*70*	*1099*
2012	34,767	51	770	35,026	78	1095
2013	19,908	53	782	19,614	78	1195
2014	28,119	59	872	19,630	71	1099
2015	*19,383**	*57**	*871**	*10,190*	*42*	*665*
2016	22,616	68	1020	23,089	68	1004
2017	39,433	68	999†	24,101	69	1002‡
2018	43,085	69	975	35,828	68	977
2019	55,586	68	953	*24,748*	*43*	*635*
2020	29,116	68	1012			

* Does not include C-license catch or effort after the C-license target for that season was switched from *D. gahi* to *Illex*.
† Includes two vessel-days of experimental fishing for juvenile toothfish.
‡ Includes one vessel-day of experimental fishing for juvenile toothfish.

Methods

The depletion model formulated for the Falklands *D. gahi* stock is based on the equivalence:

$$C_{day} = q \times E_{day} \times N_{day} \times e^{-M/2} \quad \textbf{(1)}$$

where q is the catchability coefficient, M is the natural mortality rate (considered constant at 0.0133 day^{-1}; Roa-Ureta and Arkhipkin 2007), and C_{day}, E_{day}, N_{day} are respectively catch (numbers of squid), fishing effort (numbers of vessels), and abundance (numbers of squid) per day. In its basic form (DeLury 1947) the depletion model assumes a closed population in a fixed area for the duration of the assessment. However, the assumption of a closed population is imperfectly met in the Falkland Islands fishery, where stock analyses have often shown that *D. gahi* groups arrive in successive waves after the start of the season (Roa-Ureta 2012; Winter and Arkhipkin 2015). Arrivals of successive groups are inferred from discontinuities in the catch data. Fishing on a single, closed cohort would be expected to yield gradually decreasing CPUE, but gradually increasing average individual sizes, as the squid grow. When instead these data change suddenly, or in contrast to expectation, the immigration of a new group to the population is indicated (Winter and Arkhipkin 2015).

In the event of a new group arrival, the depletion calculation must be modified to account for this influx. This is done using a simultaneous algorithm that adds new arrivals on top of the stock previously present, and posits a common catchability coefficient for the entire depletion time-series. If two depletions are included in the same model (i.e., the stock present from the start plus a new group arrival), then:

$$C_{day} = q \times E_{day} \times (N1_{day} + (N2_{day} \times i2\big|_0^1)) \times e^{-M/2} \quad \textbf{(2)}$$

where i2 is a dummy variable taking the values 0 or 1 if 'day' is before or after the start day of the second depletion. For more than two depletions, $N3_{day}$, i3, $N4_{day}$, i4, etc., would be included following the same pattern.

In several previous seasons since second season 2017 (Winter 2017), the depletion equation **(2)** was further modified to differentiate between catches taken with or without SEDs installed in the trawl nets. However, an analysis computed last year (Winter 2019a) found that daily biomass estimation did not change significantly between implementation or not of SED differentiation, and this modification was discontinued (Winter 2019b). All catch efficiencies, with or without SED, are considered part of the fleet's overall range of variation.

The season depletion likelihood function was calculated as the difference between actual catch numbers reported and catch numbers predicted from the model (Equation **2**), statistically corrected by a factor relating to the number of days of the depletion period (Roa-Ureta 2012):

$$\text{minimization} \rightarrow \left(\left(n\text{Days - }2\right)/2\right) \times \log\left(\sum_{days}\left(\log\left(\text{predicted } C_{day}\right) - \log\left(\text{actual } C_{day}\right)\right)^2\right) \quad \textbf{(3)}$$

The stock assessment was set in a Bayesian framework (Punt and Hilborn 1997), whereby results of the season depletion model are conditioned by prior information on the stock; in this case the information from the pre-season survey.

The likelihood function of prior information was calculated as the normal distribution of the difference between catchability (q) derived from the survey abundance estimate, and catchability derived from the season depletion model. Applying this difference requires both the survey and the season to be fishing the same stock with the same gear. Catchability, rather than abundance N, is used for calculating prior likelihood because catchability informs the entire season time series; whereas N from the survey only informs the first in-season depletion period – subsequent immigrations and depletions are independent of the abundance that was present during the survey. Thus, the prior likelihood function was:

$$\text{minimization} \rightarrow \frac{1}{\sqrt{2\pi \cdot SD_{q\ prior}^{2}}} \times \exp\left(-\frac{\left(q_{model} - q_{prior}\right)^{2}}{2 \cdot SD_{q\ prior}^{2}}\right) \quad \textbf{(4)}$$

where the standard deviation of catchability prior ($SD_{q\ prior}$) was calculated from the Euclidean sum of the survey prior estimate uncertainty, the variability in catches on the season start date, and the uncertainty in the natural mortality M estimate over the number of days mortality discounting (Appendix: Equations **A5-S**, **A5-N**).

Bayesian optimization of the depletion was calculated by jointly minimizing Equations **3** and **4**, using the Nelder-Mead algorithm in R programming package 'optimx' (Nash and Varadhan 2011). Relative weights in the joint optimization were assigned to Equations **3** and **4** as the converse of their coefficients of variation (CV), i.e., the CV of the prior became the weight of the depletion model and the CV of the depletion model became the weight of the prior. Calculations of the depletion CVs are described in Equations **A8-S** and **A8-N**. Because a complex model with multiple depletions may converge on a local minimum rather than global minimum, the optimization was stabilized by running a feed-back loop that set the q and N parameter outputs of the Bayesian joint optimization back into the in-season-only minimization (Equation **3**), re-calculated this minimization and the CV resulting from it, then re-calculated the Bayesian joint optimization, and continued this process until both the in-season minimization and the joint optimization remained unchanged.

With actual C_{day}, E_{day} and M being fixed parameters, the optimization of Equation **2** using Equations **3** and **4** produces estimates of q and N1, N2, …, etc. Numbers of squid on the final day (or any other day) of a time series are then calculated as the numbers N of the depletion start days discounted for natural mortality during the intervening period, and subtracting cumulative catch also discounted for natural mortality (CNMD). Taking for example a two-depletion period:

$$\begin{aligned} N_{final\ day} \quad = \quad & N1_{start\ day\ 1} \times e^{-M\ (final\ day - start\ day\ 1)} \\ & + N2_{start\ day\ 2} \times e^{-M\ (final\ day - start\ day\ 2)} \\ & - CNMD_{final\ day} \end{aligned} \quad \textbf{(5)}$$

where

$$CNMD_{day\ 1} \quad = \quad 0$$

$$CNMD_{day\ x} \quad = \quad CNMD_{day\ x\text{-}1} \times e^{-M} + C_{day\ x\text{-}1} \times e^{-M/2} \quad \textbf{(6)}$$

$N_{final\ day}$ is then multiplied by the average individual weight of squid on the final day to give biomass. Daily average individual weight is obtained from length / weight conversion of mantle lengths measured in-season by observers, and also derived from in-season commercial data as the proportion of product weight that vessels reported per market size category. Observer mantle lengths are scientifically accurate, but restricted to 1-2 vessels at any one time that may or may not be representative of the entire fleet, and not available every day. Commercially proportioned mantle lengths are relatively less accurate, but cover the entire fishing fleet every day. Therefore, both sources of data are used (see Appendix – *Doryteuthis gahi* individual weights).

Distributions of the likelihood estimates from joint optimization (i.e., measures of their statistical uncertainty) were computed using a Markov Chain Monte Carlo (MCMC) (Gamerman and Lopes 2006), a method that is commonly employed for fisheries assessments (Magnusson et al. 2013). MCMC is an iterative process which generates random stepwise changes to the proposed outcome of a model (in this case, the q and N of *D. gahi* squid) and at each step, accepts or nullifies the change with a probability equivalent to how well the change fits the model parameters compared to the previous step. The resulting sequence of accepted or nullified changes (i.e., the 'chain') approximates the likelihood distribution of the model outcome. The MCMC of the depletion models were run for 200,000 iterations; the first 1000 iterations were discarded as burn-in sections (initial phases over which the algorithm stabilizes); and the chains were thinned by a factor equivalent to the maximum of either 5 or the inverse of the acceptance rate (e.g., if the acceptance rate was 12.5%, then every 8th (0.125^{-1}) iteration was retained) to reduce serial correlation. For each model three chains were run; one chain initiated with the parameter values obtained from the joint optimization of Equations **3** and **4**, one chain initiated with these parameters ×2, and one chain initiated with these parameters ×¼. Convergence of the three chains was accepted if the variance among chains was less than 10% higher than the variance within chains (Brooks and Gelman 1998). When convergence was satisfied the three chains were combined as one final set. Equations **5**, **6**, and the multiplication by average individual weight were applied to the CNMD and each iteration of N values in the final set, and the biomass outcomes from these calculations represent the distribution of the estimate. The peaks of the MCMC histograms were compared to the empirical optimizations of the N values.

Depletion models and likelihood distributions were calculated separately for north and south sub-areas of the Loligo Box fishing zone, as *D. gahi* sub-stocks emigrate from different spawning grounds and remain to an extent segregated (Arkhipkin and Middleton 2002). Total escapement biomass is then defined as the aggregate biomass of *D. gahi* on the last day of the season for north and south sub-areas combined. North and south biomasses are not assumed to be uncorrelated however (Shaw et al. 2004), and therefore north and south likelihood distributions were added semi-randomly in proportion to the strength of their day-to-day correlation (see Winter 2014, for the semi-randomization algorithm).

Stock assessment

Data

The north sub-area was fished on 39 of the 68 season-days, for 25.1% of the total catch (7311.8 t *D. gahi*) and 27.8% of the effort (281.4 vessel-days) (Figures 3 and 4). 31.0% of north catch was taken in the 6-day period from February 28th to March 4th, and 64.4% of north catch was taken in the 21-day period from April 2nd to April 22nd (Figure 4). The south sub-area was fished on 62 of the 68 season-days, for 74.9% of total catch (21804.3 t *D. gahi*) and 72.2% of effort (730.6 vessel-days). In this season the distribution of *D. gahi* catch was conspicuously centric (Figure 3), with 9.2% of total catch and some of the heaviest trawls taken between 52°S and 52.5°S; the historically defined central sub-area of the Loligo Box (e.g., Figure 2 in Roa-Ureta and Arkhipkin 2007).

1012 vessel-days were fished during the season (Table 1), with a median of 16 vessels per day (mean 15.28) except for flex and weather extensions. Vessels reported daily catch totals to the FIFD and electronic logbook data that included trawl times, positions, depths, and product weight by market size categories. Three FIG fishery observers were deployed in the fishing season for a total of 66 sampling days[a] (Guest 2020, Roberts 2020, Tutjavi 2020). Throughout the 68 days of the season, 18 days had no FIG fishery observer covering (including 1 of the 3 season-end extension days), 35 days had 1 FIG fishery observer covering, 14 days had two FIG fishery observers covering, and 1 day had three FIG observers covering. Except for seabird days FIG fishery observers were tasked with sampling 200 *D.*

[a] Not counting seabird days (every fourth day).

gahi at two stations; reporting their maturity stages, sex, and lengths to 0.5 cm. Contract marine mammal monitors were tasked with measuring 200 unsexed lengths of *D. gahi* per day. The length-weight relationship for converting observer and commercially proportioned lengths was combined from 1st pre-season and season length-weight data of both 2019 and 2020, as 2020 data became available progressively with on-going observer coverage. The final parameterization of the length-weight relationship included 3198 measures from 2019 and 1710 measures from 2020, giving:

$$\text{weight (kg)} = 0.26972 \times \text{length (cm)}^{2.04604} / 1000 \quad \textbf{(7)}$$

with a coefficient of determination R^2 = 87.6%.

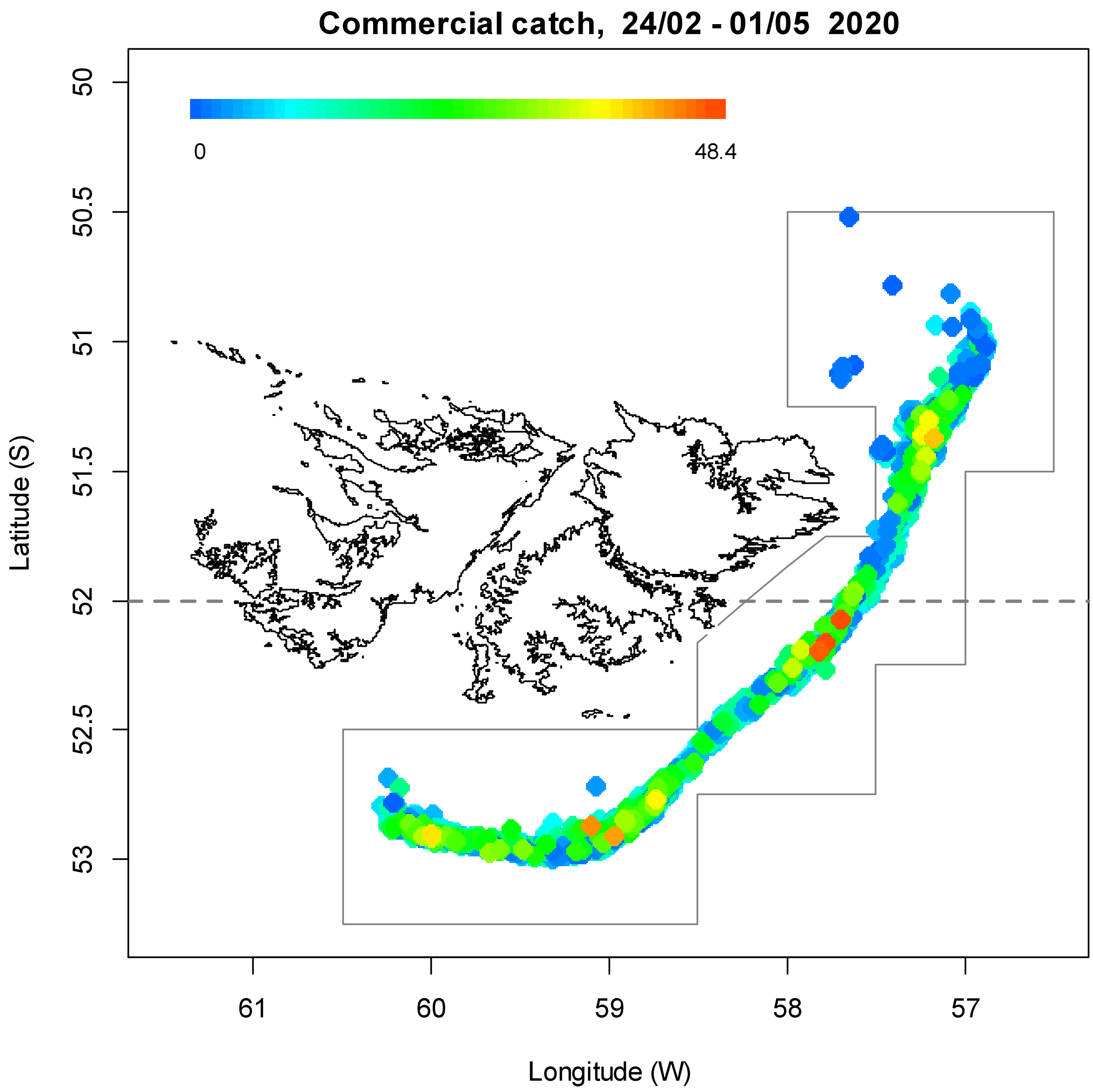

Figure 3. Spatial distribution of *D. gahi* 1st-season trawls, colour-scaled to catch weight (max. = 48.4 tonnes). 2570 trawl catches were taken during the season. The ‘Loligo Box’ fishing zone and 52 ºS parallel delineating the boundary between north and south assessment sub-areas, are shown in grey.

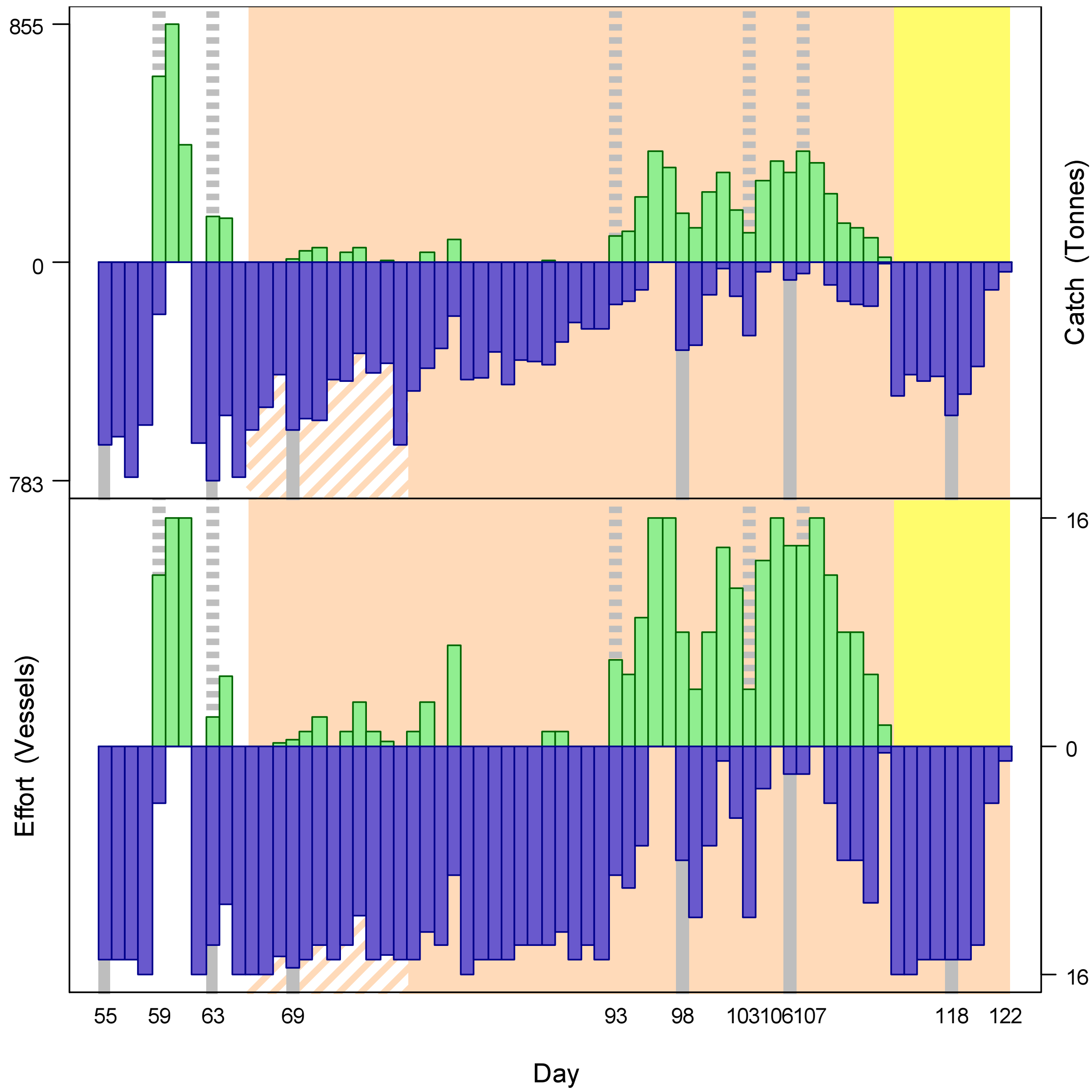

Figure 4. Daily total *D. gahi* catch and effort distribution by assessment sub-area north (green) and south (purple) of the 52° S parallel during 1st season 2020. The season was open from February 24th (chronological day 55) to April 28th (chronological day 119), plus flex days until May 1st (day 122). Orange under-shading delineates the mandatory use of SEDs north and south; the striated under-shading denotes that SEDs had been mandated south to 52.25° S; i.e., partially into the southern sub-area. Yellow under-shading delineates the early closure of the north sub-area. As many as 16 vessels fished per day north; as many as 16 vessels fished per day south. As much as 855 tonnes *D. gahi* was caught per day north; as much as 783 tonnes *D. gahi* was caught per day south.

Group arrivals / depletion criteria

Start days of depletions - following arrivals of new *D. gahi* groups - were judged primarily by daily changes in CPUE, with additional information from sex proportions, maturity, and average individual squid sizes. CPUE was calculated as metric tonnes of *D. gahi* caught per vessel per day. Days were used rather than trawl hours as the basic unit of effort. Commercial vessels do not trawl standardized duration hours, but rather durations that best suit their daily processing requirements. An effort index of days is therefore more consistent.

Six days in the south and five days in the north were identified that represented the onset of separate immigrations / depletions throughout the season.

- The first depletion start south was set on day 55 (February 24th), the first day of the season with all vessels fishing south. Average individual weight and maturity (observer measured) showed increasing trends (Figures 5B and D).
- The second depletion start south was identified on day 63 (March 3rd), with the season's highest CPUE south (Figure 6) and starting increases of average individual weight (commercial and observer) and maturity (Figures 5A, B and D).
- The third depletion start south was identified on day 69 (March 9th) with an increase in CPUE after 7 days decreasing trend (Figure 6), and the day after minima of average individual weight (commercial and observer), and proportion female (Figures 5A, B, C).
- The fourth depletion start south was identified on day 98 (April 7th) with a CPUE peak fished by 8 vessels (following two days during which no effort had been taken south; Figure 6). Average individual weights were high according to commercial distributions and mid-range according to observer measurements, while the proportion of females was the lowest for the remainder of the season (Figures 5A, B and C).
- The fifth depletion start south was identified on day 106 (April 15th) with a CPUE peak; albeit fished by only 2 vessels following a day of no fishing in the south (Figure 6), and low average individual observer weight (Figure 5B).
- The sixth depletion start south was identified on day 118 (April 27th) with a strong CPUE peak (Figure 6) and local minima or near-minima of average individual weight (commercial and observer measured), proportion female, and maturity (Figure 5).
- The first depletion start north was set on day 59 (February 28th), the first day of fishing in the north sub-area, by twelve vessels. CPUE was second-highest for the season (Figure 6), while average maturity was the lowest it would be all season in the north (Figure 5D).
- The second depletion start north was identified on day 63 (March 3rd) with the season-highest peak of CPUE which was, however, fished by only two vessels (Figure 6). The proportion of females was sharply lower than either the last measured day before or after (Figure 5C).
- The third depletion start north was identified on day 93 (April 2nd), the first day that the north had been fished by more than a single vessel since March 21st (Figure 6). Assignment of a depletion start to this day was therefore effectively by default. Average individual weights (commercial and observer measured) showed local minima (Figures 5A and B).
- The fourth depletion start north was identified on day 103 (April 12th) with a modest CPUE peak (Figure 6) and local minima of average individual weights (commercial and observer measured) (Figures 5A and B).
- The fifth depletion start north was identified on day 107 (April 16th) with a CPUE peak fished by 14 vessels (Figure 6) and prominent minima of average individual weights (commercial and observer measured) (Figures 5A and B).

Figure 5 [next page]. A: Average individual *D. gahi* weights (kg) per day from commercial size categories. B: Average individual *D. gahi* weights (kg) by sex per day from observer sampling. C: Proportions of female *D. gahi* per day from observer sampling. D: Average maturity value by sex per day from observer sampling. Males: triangles, females: squares, unsexed: circles. North sub-area: green, south sub-area: purple. Data from consecutive days are joined by line segments. Broken grey bars: the starts of in-season depletions north. Solid grey bars: the starts of in-season depletions south.

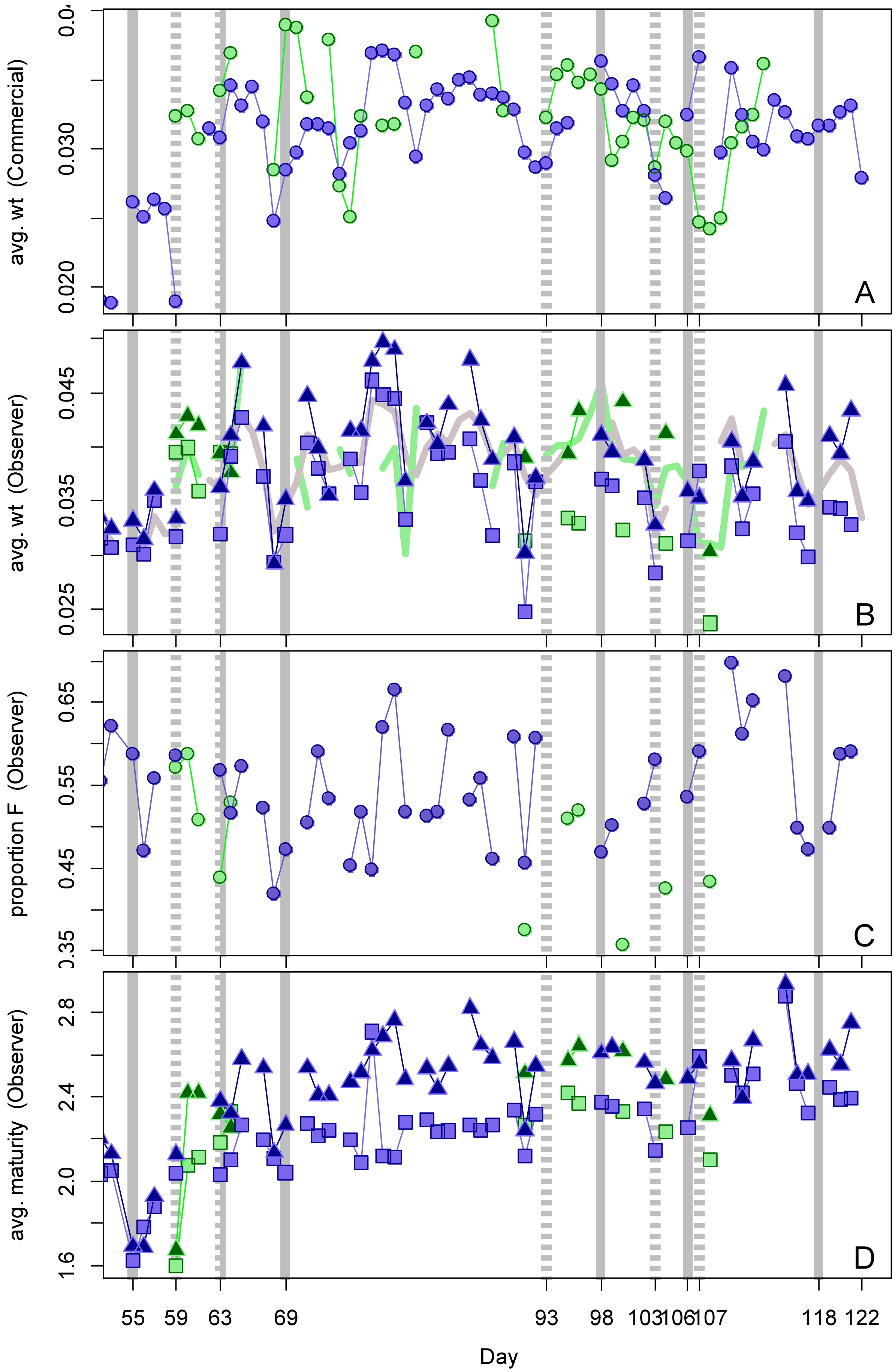
avg. wt (Commercial)
0.020
0.030
A
avg. wt (Observer)
0.025
0.035
0.045
B
proportion F (Observer)
0.35
0.45
0.55
0.65
C
avg. maturity (Observer)
1.6
2.0
2.4
2.8
D
55
59
63
69
93
98
103
106
107
118
122
Day

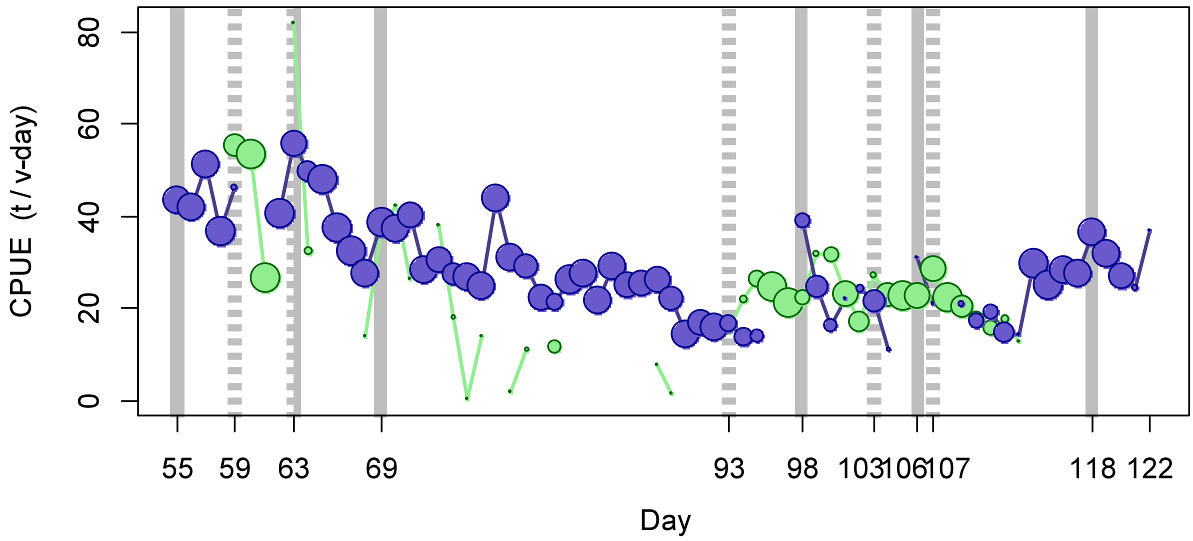

Figure 6. CPUE in metric tonnes per vessel per day, by assessment sub-area north (green) and south (purple) of 52° S latitude. Circle sizes are proportioned to numbers of vessels fishing. Data from consecutive days are joined by line segments. Broken grey bars indicate the starts of in-season depletions north. Solid grey bars indicate the starts of in-season depletions south.

Depletion analyses
South

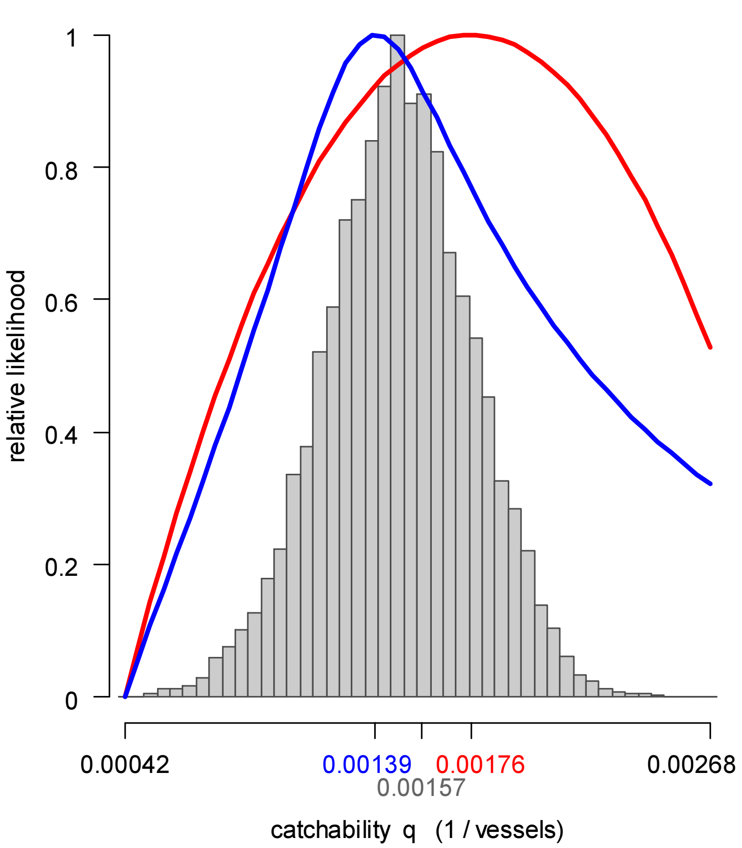

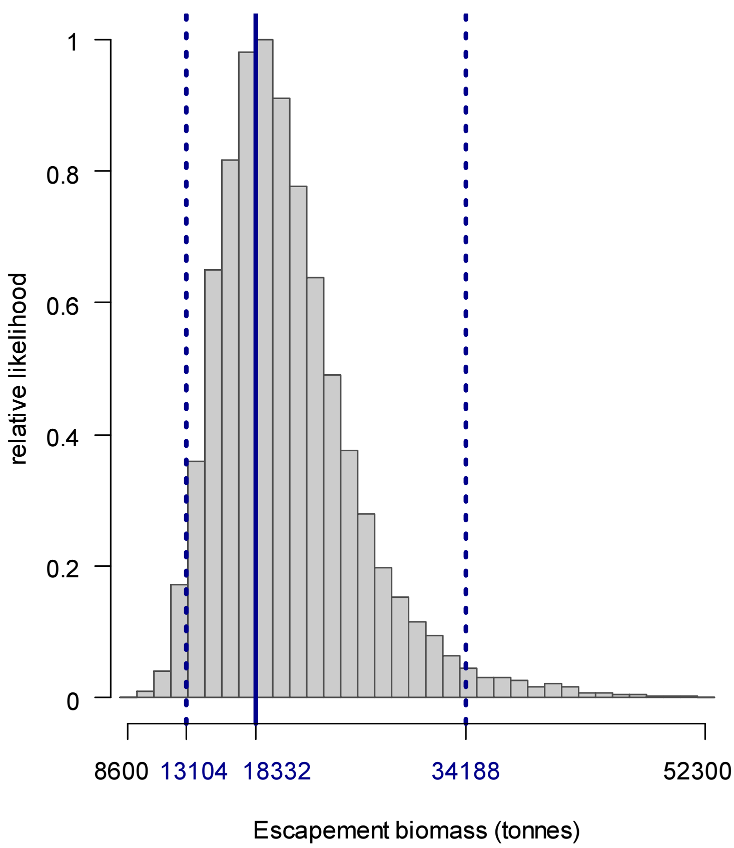

Figure 7 [previous page]. South sub-area. Left: Likelihood distributions for *D. gahi* catchability. Red line: prior model (pre-season survey data), blue line: in-season depletion model, grey bars: combined Bayesian model posterior. Right: Likelihood distribution (grey bars) of escapement biomass, from Bayesian posterior and average individual squid weight at the end of the season. Blue lines: maximum likelihood and 95% confidence interval. Note correspondence to Figure 8.

In the south sub-area, Bayesian optimization was weighted more to in-season depletion at 0.610 (**A5-S**) than to the prior at 0.214 (**A8-S**), given a well-developed depletion curve (Figure 6). Both the pre-season prior ($_{\text{prior}}\ q\ _S = 1.758 \times 10^{-3}$; Figure 7-left, and Equation **A4-S**) and the in-season depletion ($_{\text{depletion}}\ q\ _S = 1.390 \times 10^{-3}$; Figure 7-left, and **A6-S**) were in close proximity of each other, obtaining a maximum likelihood posterior ($_{\text{Bayesian}}\ q\ _S = 1.565 \times 10^{-3}$; Figure 7-left, and Equation **A9-S**) that was centred between the two.

The MCMC distribution of the Bayesian posterior multiplied by the GAM fit of average individual squid weight (Figure A1-south) gave the likelihood distribution of *D. gahi* biomass on day 122 (May 1st) shown in Figure 7-right, with maximum likelihood and 95% confidence interval of:

$B_{S\ \text{day}\ 122}$ = 18,332 t ~ 95% CI [13,104 – 34,188] t **(8-S)**

On the first day of the season estimated *D. gahi* biomass south was 27,153 t ~ 95% CI [18,676 – 38,000] t (Figure 8); statistically within range of the pre-season estimate of 20,685 t [14,754 – 31,618] (Winter et al. 2020). At its highest point (first in-season immigration: day 63 – March 3rd), estimated *D. gahi* biomass south was 29,560 t ~ 95% CI [23,202 – 44,883] t. Average biomass south decreased significantly from day 63 to day 98 (April 7th), and thereafter iteratively increased with the further immigrations, but variability after day 98 exceeded statistical significance of biomasses changes by the rule that a straight line could be drawn through the plot (Figure 8) without intersecting the 95% confidence intervals (Swartzman et al. 1992).

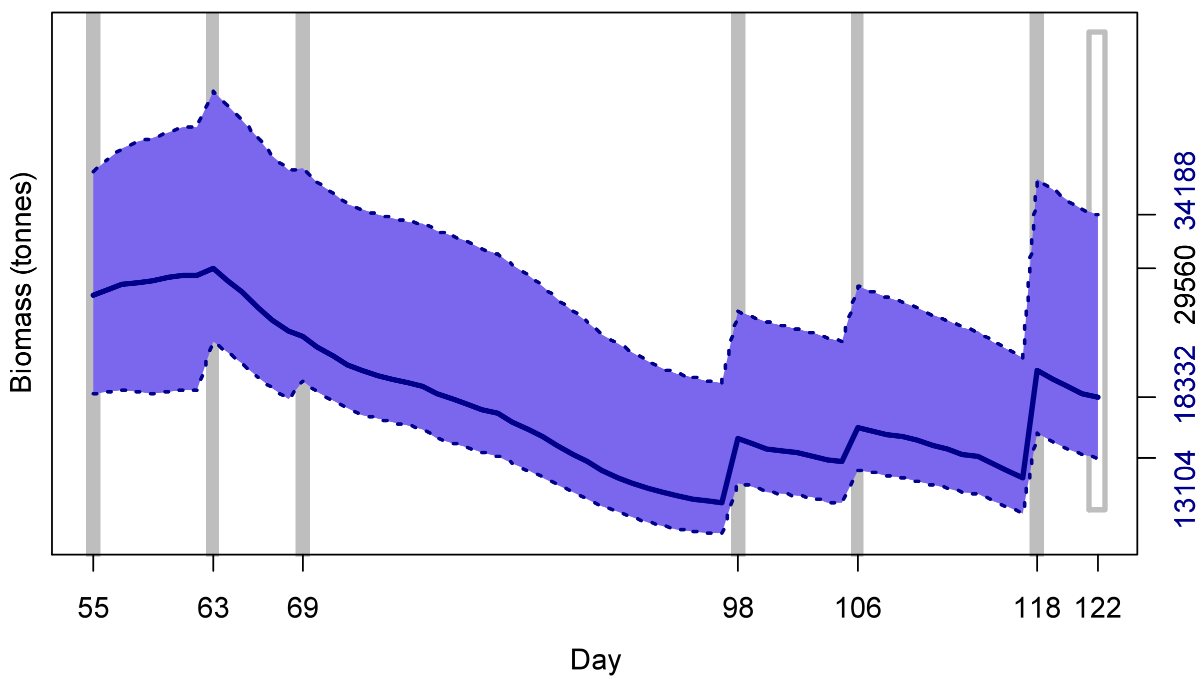

Figure 8 [previous page]. South sub-area. *D. gahi* biomass time series estimated from Bayesian posterior of the depletion model ± 95% confidence intervals. Grey bars indicate the start of in-season depletions south; days 55, 63, 69, 98, 106 and 118. Note that the biomass 'footprint' on day 122 (May 1st) corresponds to the right-side plot of Figure 7.

North

In the north sub-area, one potentially unstable outcome of model optimization was elevated values of catchability q. The pre-season prior ($_{prior}\ q\ _{N} = 8.206 \times 10^{-3}$; Figure 9-left, and Equation **A4-N**) was informed by the low pre-season survey estimate of north sub-area biomass (Winter et al. 2020) followed by briefly very high catches and CPUE at the start of the season (Figures 4 and 5). The subsequent in-season depletion was poorly defined with sparse and low catches (Figure 6), giving in-season depletion that was anomalously high ($_{depletion}\ q\ _{N} = 1.879 \times 10^{-2}$; off the scale on Figure 9-left, and Equation **A6-N**). The resulting maximum likelihood posterior ($_{Bayesian}\ q\ _{N} = 8.789 \times 10^{-3}$; Figure 9-left, and Equation **A9-N**) was consequently determined primarily by the prior, despite relatively even modelling weights: 0.805 in-season depletion (**A5-N**) vs. 0.624 prior (**A8-N**).

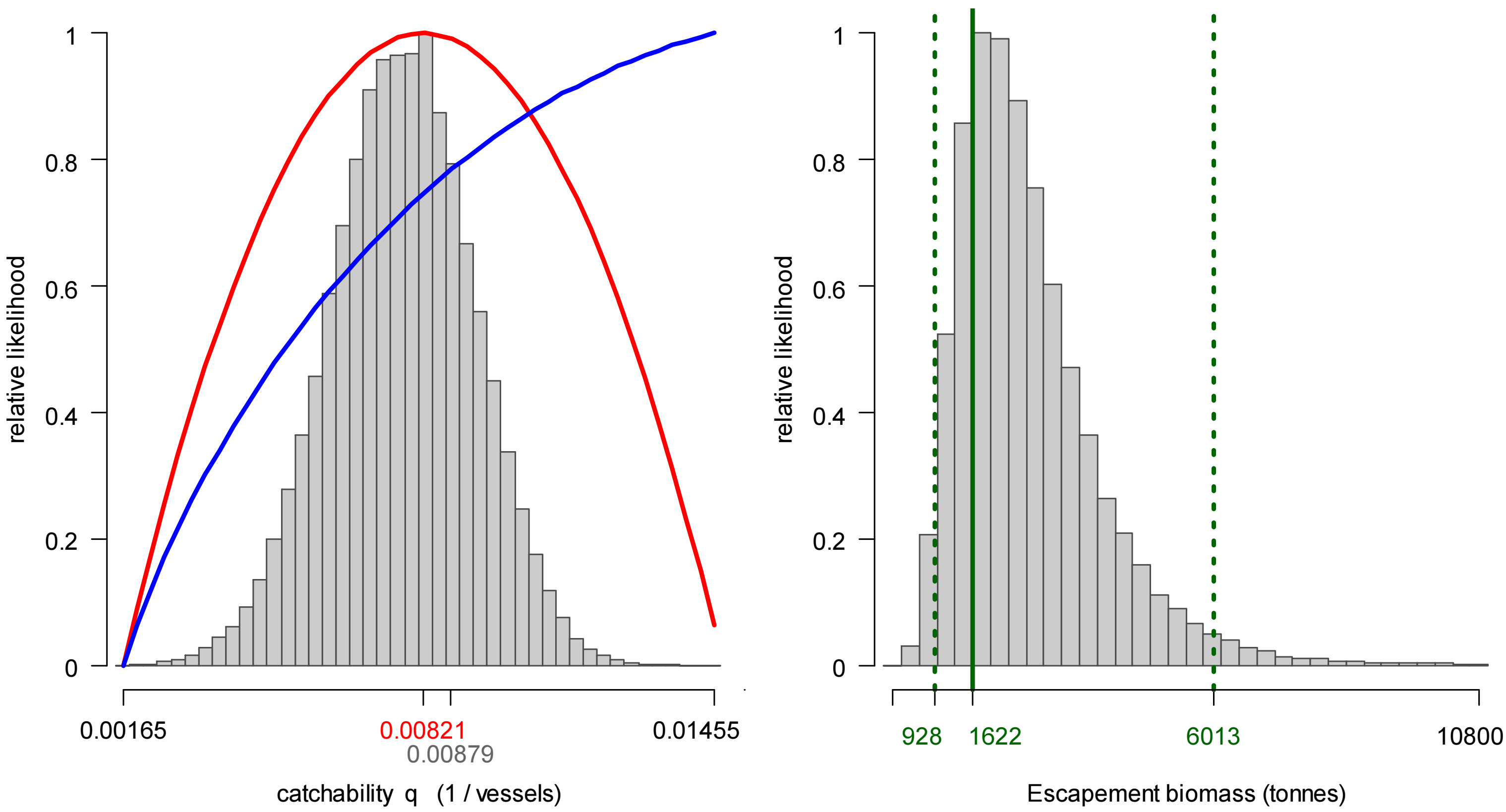

Figure 9. North sub-area. Left: Likelihood distributions for *D. gahi* catchability. Red line: prior model (pre-season survey data), blue line: in-season depletion model, grey bars: combined Bayesian model posterior. Right: Likelihood distribution (grey bars) of escapement biomass, from Bayesian posterior and average individual squid weight at the end of the season. Green lines: maximum likelihood and 95% confidence interval. Note the correspondence to Figure 10.

The MCMC distribution of the Bayesian posterior multiplied by the generalized additive model (GAM) fit of average individual squid weight (Figure A1-north) gave the likelihood distribution of *D. gahi* biomass on day 122 (May 1st) shown in Figure 9-right, with maximum likelihood and 95% confidence interval of:

$B_{\text{N day 122}}$ = 1622 t ~ 95% CI [928 – 6013] t **(8-N)**

Fishing in the north had ended on day 113 (April 22nd), but natural mortality continued slowly reducing the biomass until the overall season end (Figure 10). On the first day of fishing (day 59, February 28th) the estimated *D. gahi* biomass north was 3750 t ~ 95% CI [3298 – 5856] t (Figure 10); statistically lower than the pre-season estimate of 7306 t [6129 – 13,134] (Winter et al. 2020), which refutes the possibility that an undetected immigration might have happened between the last day a survey trawl was actually taken in the north (February 16th) and the start of commercial fishing. Estimated *D. gahi* biomass north decreased by a significant margin from day 59, then increased sharply with the immigration on day 93 (April 2nd) to its highest point of the season: 4162 t [3067 – 8067]. Biomass generally declined thereafter aside from two more small immigrations, but variability in the trend was high, precluding further statistical significance (Figure 10).

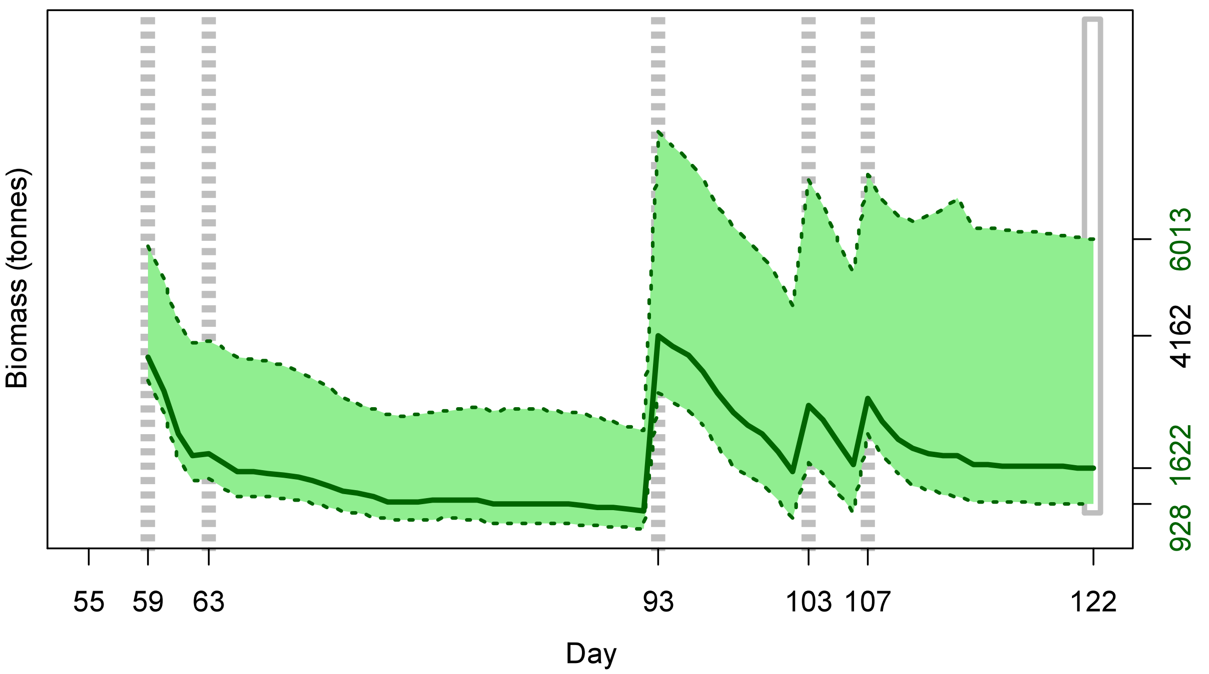

Figure 10. North sub-area. *D. gahi* biomass time series estimated from Bayesian posterior of the depletion model ± 95% confidence intervals. Broken grey bars indicate the start of in-season depletions north; days 59, 63, 93, 103 and 107. Note that the biomass 'footprint' on day 122 (May 1st) corresponds to the right-side plot of Figure 9.

Immigration

Doryteuthis gahi immigration during the season was inferred on each day by how many more squid were estimated present than the day before, minus the number caught and the number expected to have died naturally:

$$_{\text{Immigration}}N_{\text{day } i} = N_{\text{day } i} - (N_{\text{day } i-1} - C_{\text{day } i-1} - M_{\text{day } i-1})$$

where $N_{\text{day } i-1}$ are optimized in the depletion models, $C_{\text{day } i-1}$ calculated as in Equation **3**, and $M_{\text{day } i-1}$ is:

$$M_{\text{day } i-1} = (N_{\text{day } i-1} - C_{\text{day } i-1}) \times (1 - e^{-M})$$

Immigration biomass per day was then calculated as the immigration number per day multiplied by predicted average individual weight from the GAM:

$$_{\text{Immigration}}B_{\text{day } i} = {}_{\text{Immigration}}N_{\text{day } i} \times {}_{\text{GAM}}Wt_{\text{day } i}$$

All numbers N are themselves derived from the daily average individual weights, therefore the estimation automatically factors in that those squid immigrating on a given day would likely be smaller than average (because younger). Confidence intervals of the immigration estimates were calculated by applying the above algorithms to the MCMC iterations of the depletion models. Resulting total biomasses of *D. gahi* immigration north and south, up to season end (day 122), were:

$$_{\text{Immigration}}B_{\text{S season}} = 19{,}698 \text{ t} \sim 95\% \text{ CI } [16{,}815 \text{ to } 34{,}857] \text{ t} \quad \textbf{(9-S)}$$

$$_{\text{Immigration}}B_{\text{N season}} = 5{,}249 \text{ t} \sim 95\% \text{ CI } [3{,}622 \text{ to } 11{,}993] \text{ t} \quad \textbf{(9-N)}$$

Total immigration with semi-randomized addition of the confidence intervals was:

$$_{\text{Immigration}}B_{\text{Total season}} = 24{,}947 \text{ t} \sim 95\% \text{ CI } [22{,}717 \text{ to } 42{,}625] \text{ t} \quad \textbf{(9-T)}$$

In the south sub-area, the in-season peaks on days 63, 69, 98, 106, and 118 accounted for approximately 6.8%, 2.7%, 25.8%, 14.8%, and 45.0% of in-season immigration (start day 55 was de facto not an in-season immigration), consistent with the variation in time series biomass on Figure 8. In the north sub-area, the in-season peaks on days 63, 93, 103 and 107 accounted for approximately 0%, 49.7%, 21.6% and 22.3% of in-season immigration (Figure 10). The model-fit outcome that perceived immigration on day 63 actually did not 'deliver' any more squid demonstrates that indicators for immigration are not absolutely deterministic.

Escapement biomass

Total escapement biomass was defined as the aggregate biomass of *D. gahi* at the end of day 122 (May 1st) for south and north sub-areas combined (Equations **8-S** and **8-N**). Depletion models are calculated on the inference that all fishing and natural mortality are gathered at mid-day, thus a half day of mortality ($e^{-M/2}$) was added to correspond to the closure of the fishery at 23:59 (mid-night) on May 1st for the final remaining vessel: Equation **10**.

$$B_{\text{Total day 122}} = (B_{\text{S day 122}} + B_{\text{N day 122}}) \times e^{-M/2}$$

$$= 19{,}954 \text{ t} \times 0.99336$$

$$= 19{,}822 \text{ t} \sim 95\% \text{ CI } [15{,}233 - 37{,}088] \text{ t} \quad \textbf{(10)}$$

South and north biomass season time series were overall negatively correlated with each other (R = –0.133). Semi-randomized addition of these distributions with negative correlation gave the aggregate likelihood of total escapement biomass shown in Figure 11. The estimated escapement biomass of 19,822 t was the lowest since 2015, the year of the exceptional *Illex* incursion (Winter 2015). The risk of the fishery in the current season, defined as the proportion of the total escapement biomass distribution below the conservation limit of 10,000 tonnes (Agnew et al., 2002; Barton, 2002), was calculated as effectively zero.

At its lowest point of the season (day 92 – April 1st) estimated *D. gahi* biomass was 11,284 tonnes with a 13.2% distribution risk below the conservation limit of 10,000 tonnes.

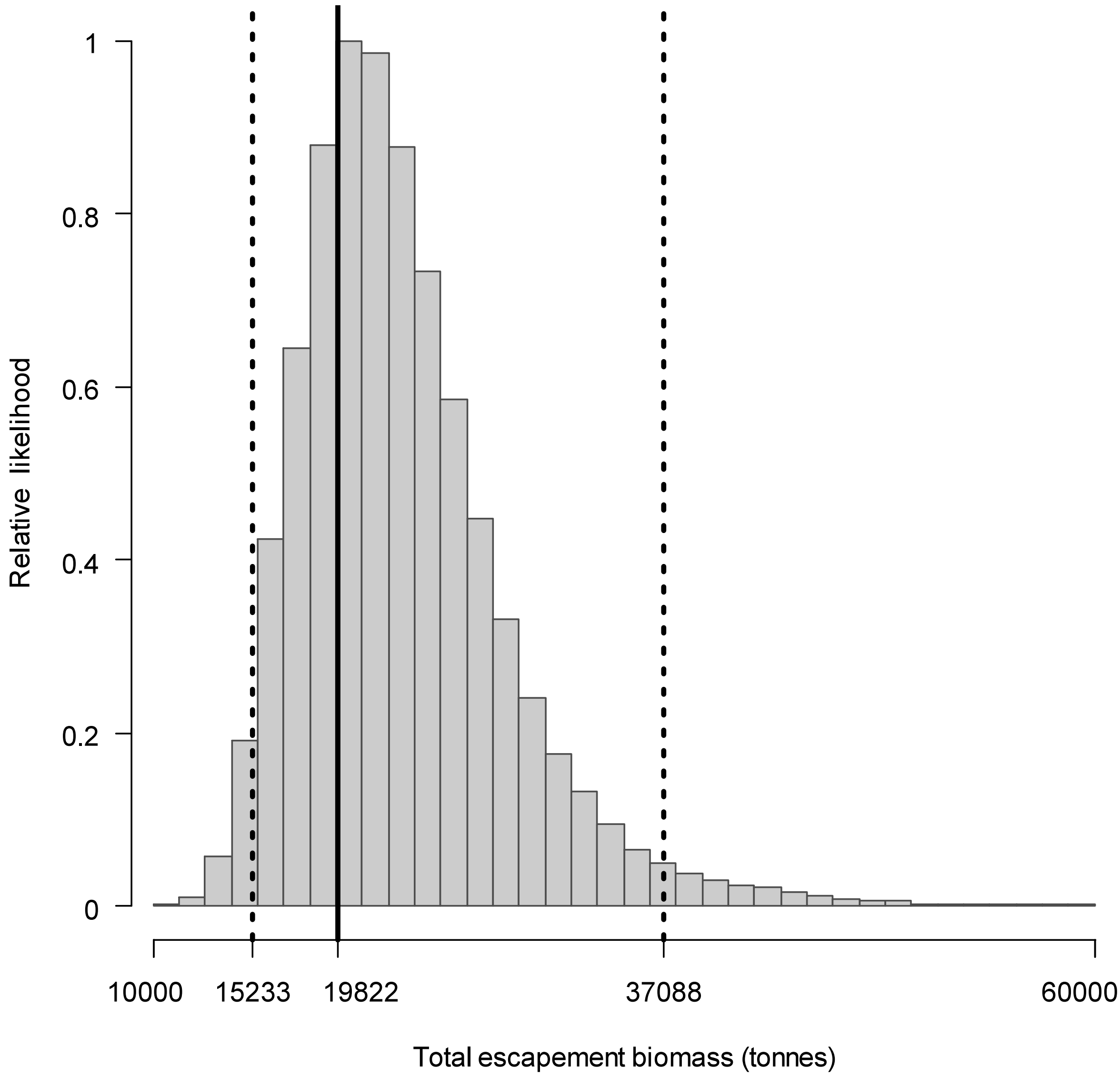

Figure 11. Likelihood distribution with 95% confidence intervals of total *D. gahi* escapement biomass at the season end (May 1st).

Pinniped bycatch

Pinniped bycatch during first season 2020 included 5 reported fishing mortalities; 1 South American fur seal (ARA - *Arctocephalus australis*) and 4 Southern sea lions (OTB - *Otaria* *flavescens*), distributed as summarized in Table 2 and Figure 12. The total reported mortality of five is the lowest since systematic marine mammal observing was started in second season 2017 (Winter 2017), and only the second time that Southern sea lion mortalities outnumbered South American fur seal mortalities, after first season 2018 (Winter 2018). The distribution of pinniped fishing mortalities was analysed for correlation with SEDs, aggregation by trawl and by vessel, daylight[b], position (latitude / longitude), trawl duration, and sea state. Correlations were tested by randomly re-distributing 100000× the pinniped mortalities among the 2570 commercial trawls during the season and calculating the proportions of the 100000 iterations that exceeded the empirical parameters[c]. The non-overlap between South American fur seal and Southern sea lion mortalities (Table 2) was also tested by these randomized re-distributions. All tests except non-overlap were calculated separately for the two pinniped species. Because the analysis implied multiple comparisons among stochastically independent null hypotheses, significance thresholds were adjusted by the Šidák correction:

$$\alpha_{corr} = 1 - (1 - \alpha)^{\frac{1}{m}} = 1 - (1 - 0.05)^{\frac{1}{5}} = 0.0102 \qquad \textbf{(11-OTB)}$$

$$\alpha_{corr} = 1 - (1 - \alpha)^{\frac{1}{m}} = 1 - (1 - 0.05)^{\frac{1}{2}} = 0.0253 \qquad \textbf{(11-ARA)}$$

where α = the standard significance threshold of p = 0.05, and m = number of independent null hypotheses: SED, daylight, position clustering, duration, sea state; thus m = five[d] for Southern sea lions and m = two[e] for South American fur seals. The analysis was restricted to mortalities as live captures are ambiguous to quantify: escapees cannot be counted accurately and the same animals may be caught repeatedly (especially if they're habituated, therefore non-independence of counts).

Table 2. Reported fishing mortalities of pinnipeds, by trawl, in 1st season 2020.

Date	Species	No.	Grid at shoot
Mar 1st	Southern sea lion	1	XQAP
Mar 5th	Southern sea lion	1	XTAM
Mar 9th	Southern sea lion	1	XUAL
Mar 17th	South American fur seal	1	XUAL
Mar 19th	Southern sea lion	1	XQAP

Results of the mortality analysis are summarized in Table 3. Pinniped mortalities were not aggregated by trawl as every South American fur seal and every Southern sea lion was

[b] Daylight is defined as a trawl hauled between sunrise and sunset, calculated using the algorithms of the NOAA Earth System research laboratory, www.esrl.noaa.gov/gmd/grad/solcalc/calcdetails.html.

[c] Either counts or weighted means.

[d] Latitude and longitude, although computed separately, were considered part of the same position parameter, therefore only one null hypothesis including both. Aggregation of trawls and vessels were tested but unlike the other parameters are not potential causative agents of mortality, therefore not part of the same 'family' of null hypotheses. As vessels are nested within trawls there was also no separate 2-fold significance correction for trawl and vessel aggregation.

[e] Given a single mortality of this species, only null hypotheses were relevant to test that a priori had an (adjusted) 5% threshold. Non-daylight was 447 out of 2570 trawls = 17.4%, non-SED was 1030 out of 2570 trawls = 40.1%; thus these two hypotheses were not tested. Position clustering, and aggregation of trawls and vessels, were also not tested for South American fur seal as a single mortality has no frame of reference against these criteria.

reported killed in a different trawl, and indeed on a different day. Pinniped mortalities were also not significantly aggregated by vessel as the four Southern sea lions were taken on three different vessels, and the South American fur seal was taken on a further different vessel. 1030 of the 2570 commercial trawls were completed before SEDs were mandated on March 6^{th} and March 18^{th}, and only one Southern sea lion mortality was reported thereafter (Table 2). No correlative null hypotheses were statistically significant at the given p-value thresholds. Only trawl duration was close to significant as the one trawl catching a South American fur seal was substantially shorter at 1.67 hours than the season average of 4.59 hours (Table 3).

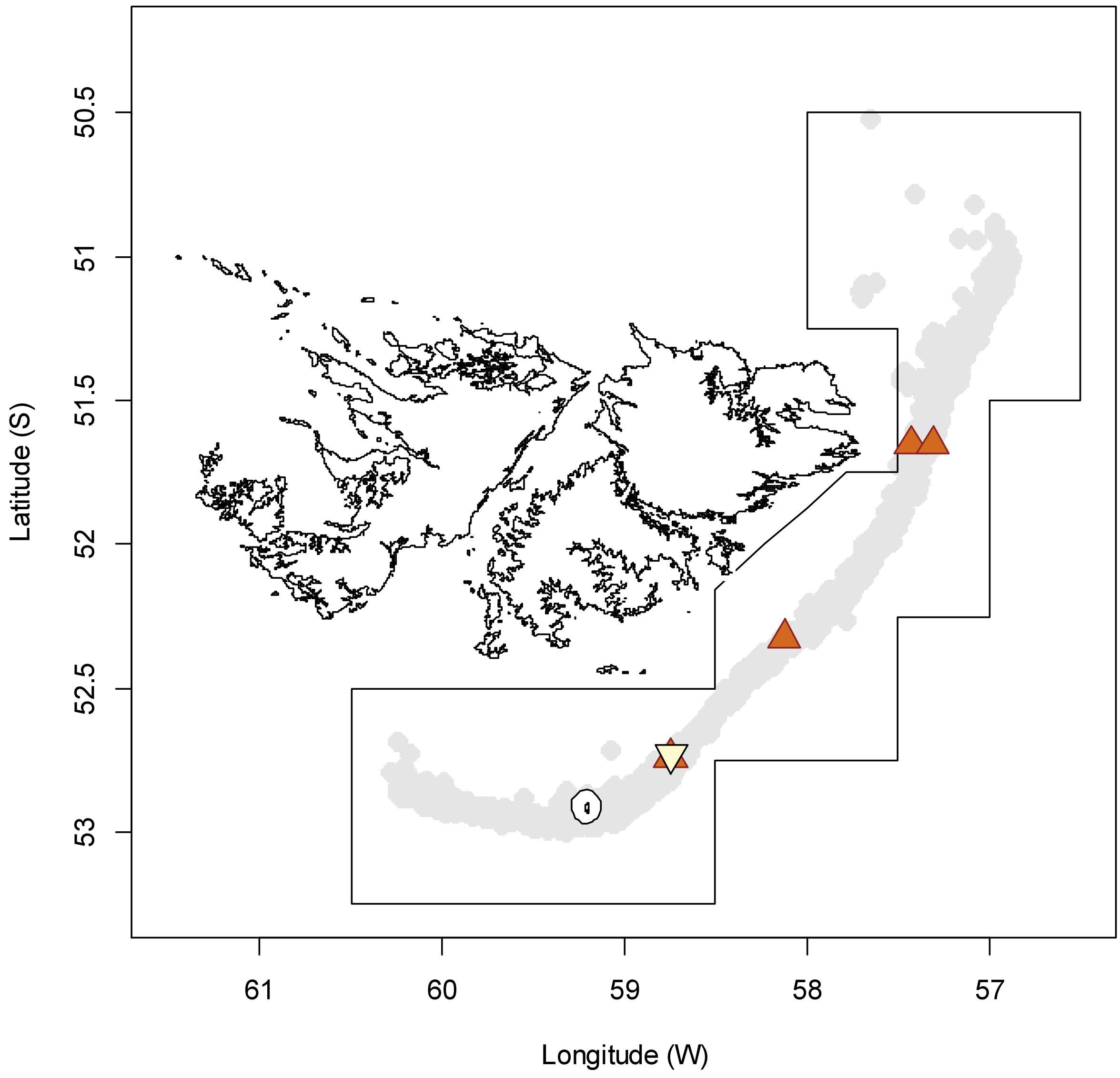

Figure 12. Distribution of pinniped mortalities during 1st season 2020, showing trawl start positions. (Mortalities may actually have occurred in either the shoot or the haul of the trawl; V. Iriarte, FIFD, pers. comm.). South American fur seals: off-white, point-down. Southern sea lions: brown, point-up. Grey under-shading: distribution of trawls, equivalent to Figure 3.

Table 3. Hypotheses correlating pinniped mortalities in the 1st season 2020 commercial fishery. Outcomes are either the mortality counts or the mortality-weighted means of that hypothesis parameter. Non-significant parameters are shaded grey.

Mortality hypothesis	South American fur seal		Southern sea lion	
	Outcome	p	Outcome	p
Trawl aggregation[a]	–	–	4 / 2570	1.000
Vessel aggregation[b]	–	–	3 / 16	>0.300
Without SED	1 / 1	–	3 / 4	>0.150
Daylight	0 / 1	–	4 / 4	>0.400
Lat / Lon position	52.73ºS × 58.74ºW	–	52.09ºS × 57.90ºW	>0.300
Trawl duration	1.67 hours	0.036	5.35 hours	>0.150
Sea state[c]	2.00	>0.120	2.50	>0.150
	Both species			
Non-overlap	0 / 5	>0.950	–	–

[a] See Table 2.
[b] Vessels not identified, for confidentiality.
[c] Beaufort wind force scale.

Fishery bycatch

Figure 13 [below]. Distributions of the eight principal bycatches during 1st season 2020, by noon position grids. Thickness of grid lines is proportional to the number of vessel-days (1 to 216 per grid; 17 different grids were occupied). Grey-scale is proportional to the bycatch biomass; maximum (tonnes) indicated on each plot.

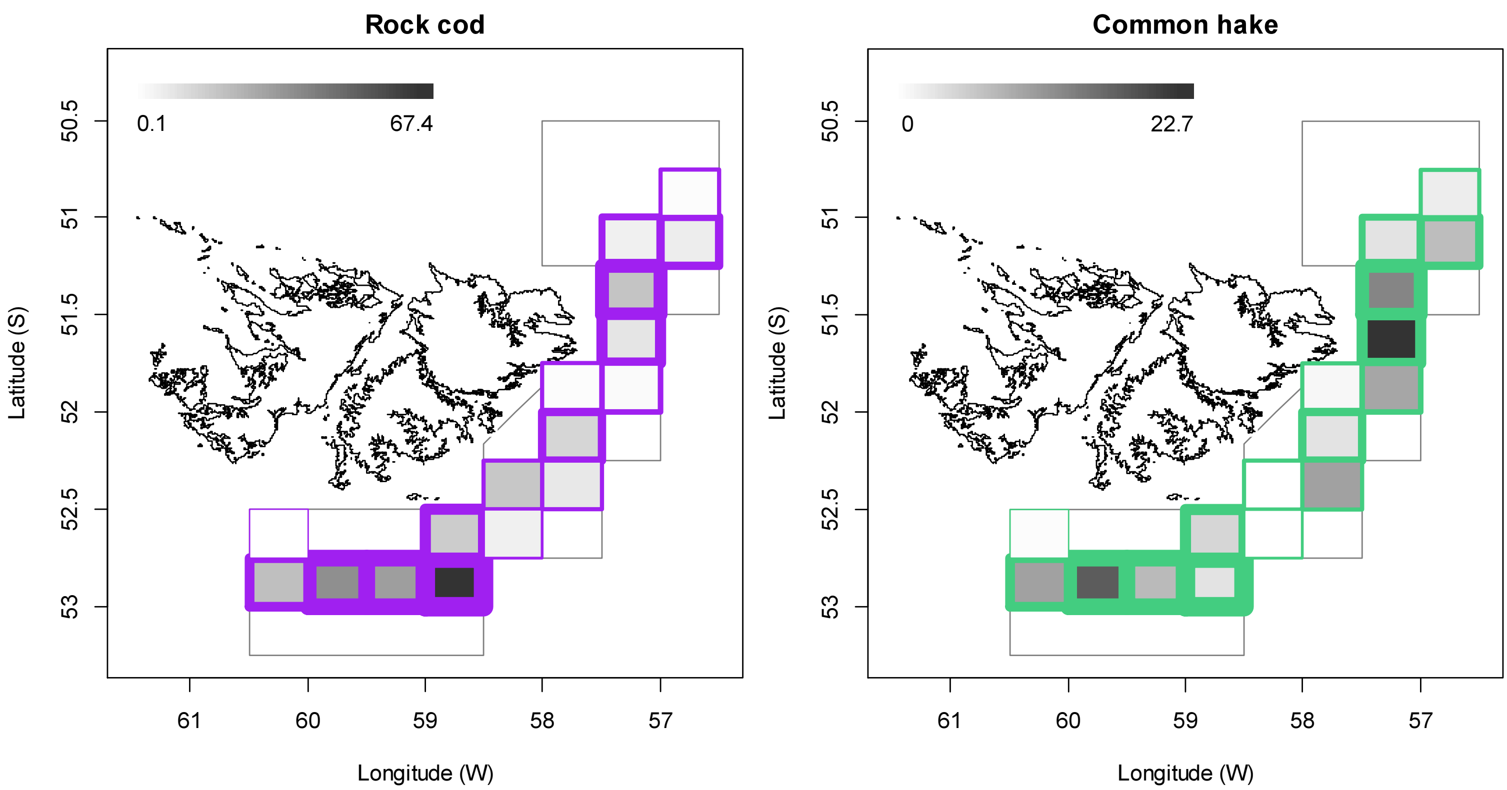

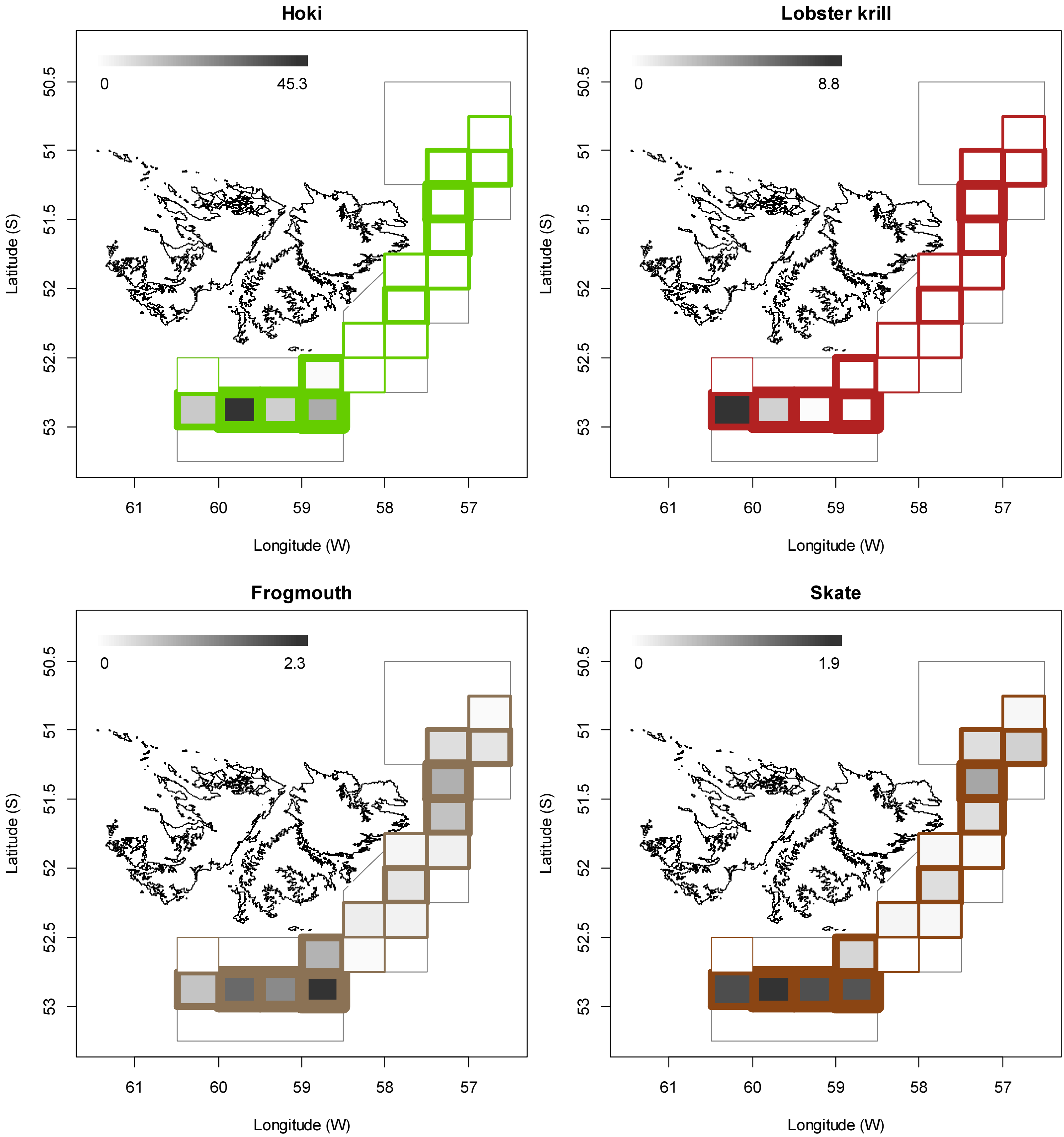
Hoki
0
45.3
Lobster krill
0
8.8
Frogmouth
0
2.3
Skate
0
1.9
Latitude (S)
50.5
51
51.5
52
52.5
53
Longitude (W)
61
60
59
58
57

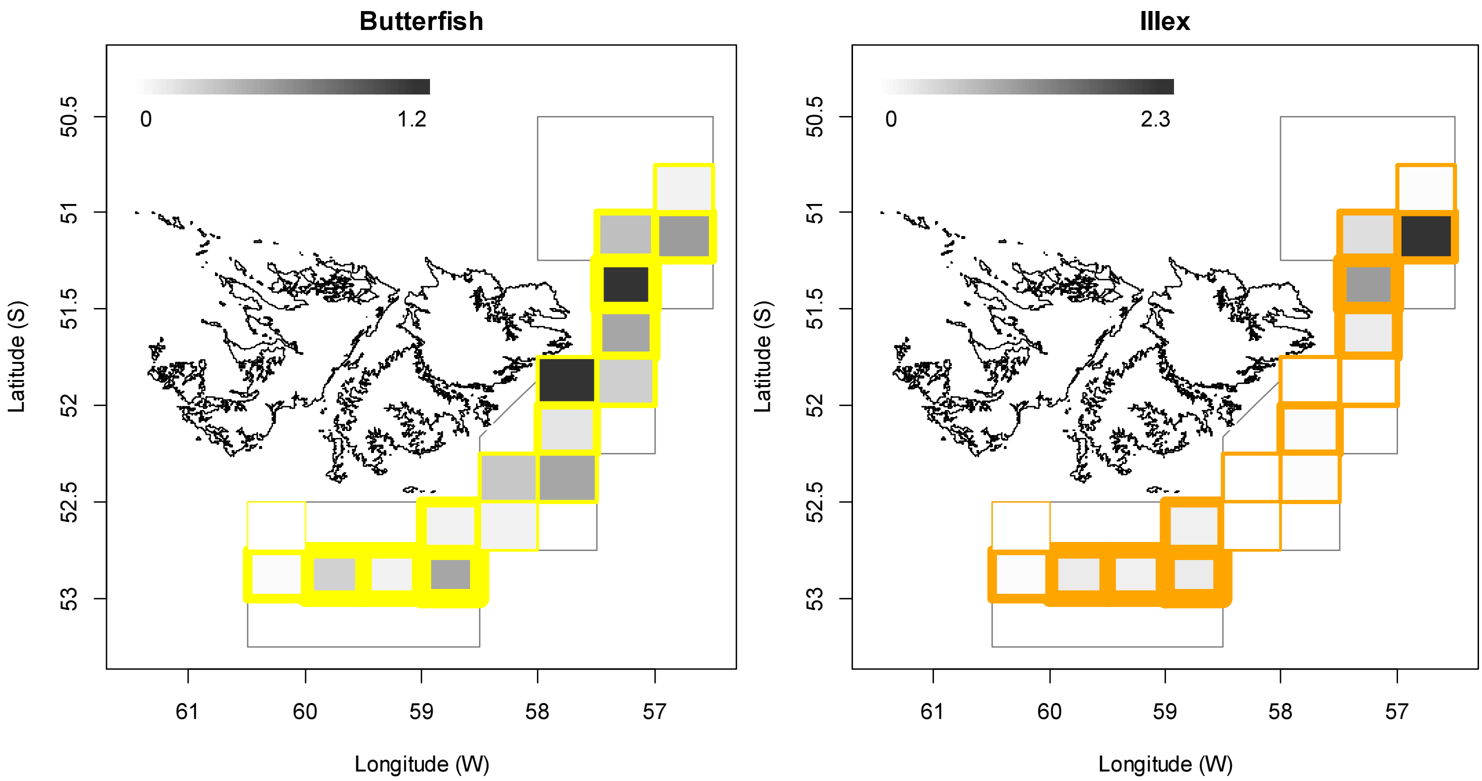

All except one of the 1012 first season vessel-days (Table 1) reported *D. gahi* squid as their primary catch. The exception was a vessel-day in the southern part of the Loligo Box that reported 56.2% hoki (*Macruronus magellanicus*) vs. 43.5% *D. gahi*. The proportion of season total catch represented by *D. gahi* (29116101/29648046 = 0.982; Table A1) is lower than both seasons last year, but above the long-term median. Highest bycatches in first season 2020 were rock cod *Patagonotothen ramsayi*, with 262 tonnes from 956 vessel-days, common hake *Merluccius hubbsi* (117 t, 404 v-days), hoki (88 t, 165 v-days), lobster krill *Munida* sp. (11 t, 67 v-days), frogmouth *Cottoperca gobio* (10 t, 595 v-days), skate Rajiformes (10 t, 505 v-days), butterfish *Stromateus brasiliensis* (7 t, 262 v-days), and shortfin squid *Illex argentinus* (5 t, 237 v-days). Relative distributions by grid of these bycatches are shown in Figure 13; the complete list of all catches by species is in Table A1.

Trawl area coverage

The impact of bottom trawling on seafloor habitat has been a matter of concern in commercial fisheries (Kaiser et al. 2002; 2006), whereby the potential severity of impact relates to spatial and temporal extents of trawling (Piet and Hintzen 2012, Gerritsen et al. 2013). For the *D. gahi* fishery, available catch, effort, and positional data are used to summarize the estimated 'ground' area coverage occupied during the season of trawling.

The procedure for summarizing trawl area coverage is described in the Appendix of the second season 2019 report (Winter 2019b). In first season 2020 50% of total *D. gahi* catch was taken from 1.9% of the total area of the Loligo Box, corresponding approximately[f]

[f] However, not exactly. There is an expected strong correlation between the density of *D. gahi* catch taken from area units and how often these area units were trawled, but the correlation is not perfectly monotonic.

to the aggregate of grounds trawled ≥8.1 times. 90% of total *D. gahi* catch was taken from 8.0% of the total area of the Loligo Box, corresponding approximately to the aggregate of grounds trawled ≥2.4 times. 100% of total *D. gahi* catch over the season was taken from 12.0% of the total area of the Loligo Box, obviously corresponding to the aggregate of all grounds trawled at least once (Figure 14 - left). Averaged by 5 × 5 km grid (Figure 14 - right), 9 grids (out of 1383) had coverage of 10 or more (that is to say, every patch of ground within that 5 × 5 km was on average trawled over 10 times or more). Thirty-nine grids had coverage of 5 or more, and 91 grids had coverage of 2 or more.

The concentration of all *D. gahi* catch into 12.0% of area is similar to the 11.7% concentration obtained in second season 2019, which was closed by emergency order (Winter 2019b). In contrast the two seasons analysed before had substantially higher concentrations (lower percentages): first season 2018 – 7.1%, and first season 2019 – 7.7%; both of which reported higher catches and escapement biomass (Winter 2018, Winter 2019a). Results continue to indicate direct correlation with fishing success: in low biomass seasons vessels cover more ground searching.

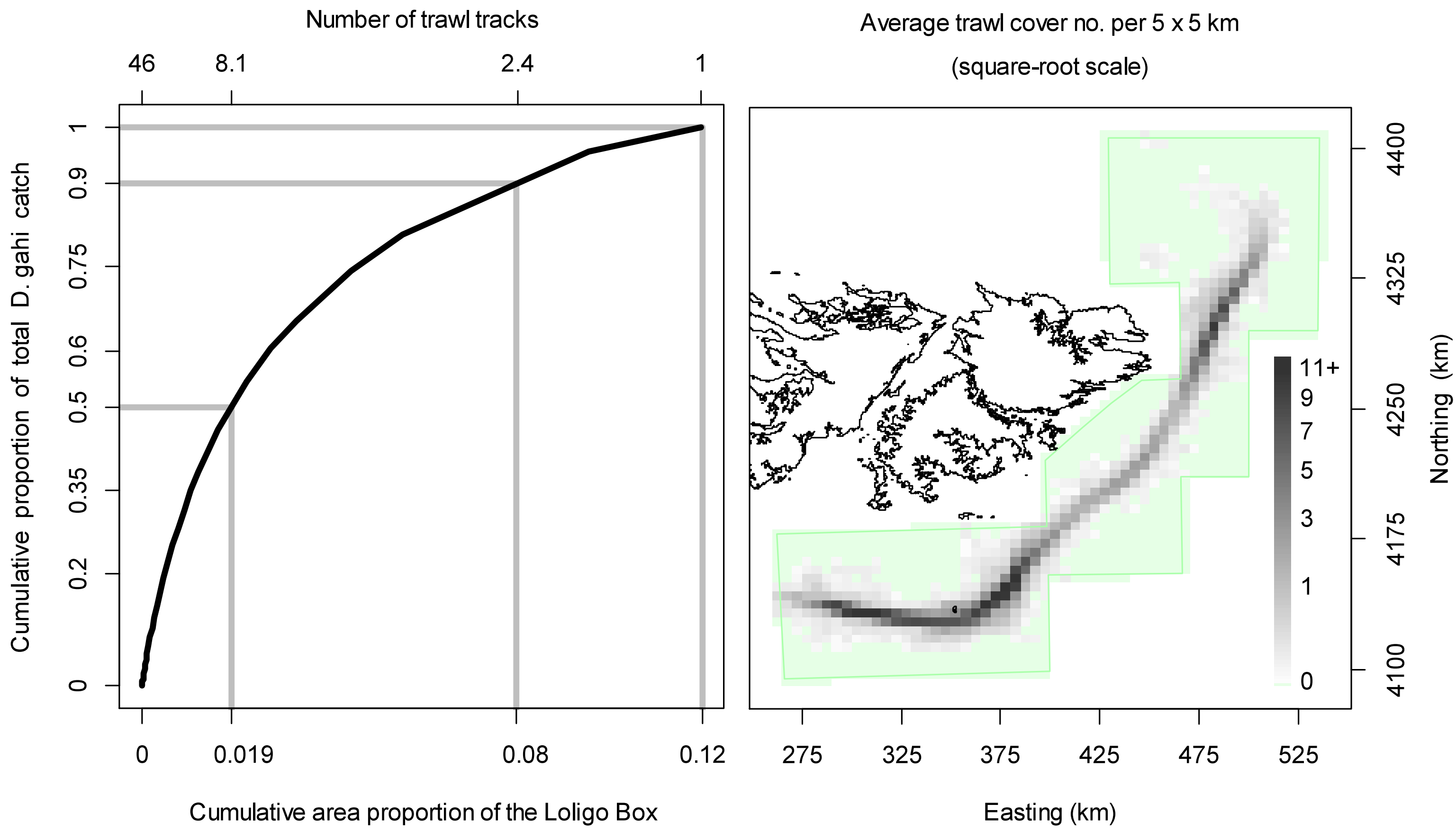

Figure 14. Left: cumulative *D. gahi* catch of 1st season 2020, vs. cumulative area proportion of the Loligo Box the catch was taken from. The maximum number of times that any single area unit was trawled was 46, and catch cumulation by reverse density corresponded approximately to the trawl multiples shown on the top x-axis. Right: trawl cover averaged by 5 × 5 km grid; green area represents zero trawling.

References

Agnew, D.J., Baranowski, R., Beddington, J.R., des Clers, S., Nolan, C.P. 1998. Approaches to assessing stocks of *Loligo gahi* around the Falkland Islands. Fisheries Research 35: 155-169.

Agnew, D. J., Beddington, J. R., and Hill, S. 2002. The potential use of environmental information to manage squid stocks. Canadian Journal of Fisheries and Aquatic Sciences, 59: 1851–1857.

Arkhipkin, A. 1993. Statolith microstructure and maximum age of *Loligo gahi* (Myopsida: Loliginidae) on the Patagonian Shelf. Journal of the Marine Biological Association of the UK 73: 979-982.

Arkhipkin, A.I., Middleton, D.A.J. 2002. Sexual segregation in ontogenetic migrations by the squid *Loligo gahi* around the Falkland Islands. Bulletin of Marine Science 71: 109-127.

Arkhipkin, A.I., Middleton, D.A.J., Barton, J. 2008. Management and conservation of a short-lived fishery resource: *Loligo gahi* around the Falkland Islands. American Fisheries Society Symposium 49: 1243-1252.

Arkhipkin, A.I., Hendrickson, L.C., Payá, I., Pierce, G.J., Roa-Ureta, R.H., Robin, J.-P., Winter, A. 2020. Stock assessment and management of cephalopods: advances and challenges for short-lived fishery resources. ICES Journal of Marine Science, doi:10.1093/icesjms/fsaa038.

Barton, J. 2002. Fisheries and fisheries management in Falkland Islands Conservation Zones. Aquatic Conservation: Marine and Freshwater Ecosystems 12: 127–135.

Brooks, S.P., Gelman, A. 1998. General methods for monitoring convergence of iterative simulations. Journal of computational and graphical statistics 7:434-455.

DeLury, D.B. 1947. On the estimation of biological populations. Biometrics 3: 145-167.

FIFD / LPG 2017. Loligo vessel substitution and other rules. Memorandum of understanding between the Falkland Islands Fisheries Department and the Loligo Producers Group, March 2017.

Gamerman, D., Lopes, H.F. 2006. Markov Chain Monte Carlo. Stochastic simulation for Bayesian inference. 2nd edition. Chapman & Hall/CRC.

Gerritsen, H.D., Minto, C., Lordan, C. 2013. How much of the seabed is impacted by mobile fishing gear? Absolute estimates from Vessel Monitoring System (VMS) point data. ICES Journal of Marine Science 70: 523-531.

Guest, A. 2020. Observer Report 1251. Technical Document, FIG Fisheries Department. 30 p.

Hoenig, J.M. 1983. Empirical use of longevity data to estimate mortality rates. Fishery Bulletin 82: 898-903

Iriarte, V., Arkhipkin, A., Blake, D. 2020. Implementation of exclusion devices to mitigate seal (*Arctocephalus australis*, *Otaria flavescens*) incidental mortalities during bottom-trawling in the Falkland Islands (Southwest Atlantic). Fisheries Research 227: 105537, 12 p.

Kaiser, M.J., Collie, J.S., Hall, S.J., Jennings, S., Poiner, I.R. 2002. Modification of marine habitats by trawling activities: prognosis and solutions. Fish and Fisheries 3: 114-136.

Kaiser, M.J., Clarke, K.R., Hinz, H., Austen, M.C.V., Somerfield, P.J., Karakassis, I. 2006. Global analysis of response and recovery of benthic biota to fishing. Marine Ecology Progress Series 311: 1-14.

Magnusson, A., Punt, A., Hilborn, R. 2013. Measuring uncertainty in fisheries stock assessment: the delta method, bootstrap, and MCMC. Fish and Fisheries 14: 325-342.

Nash, J.C., Varadhan, R. 2011. optimx: A replacement and extension of the optim() function. R package version 2011-2.27. http://CRAN.R-project.org/package=optimx

Patterson, K.R. 1988. Life history of Patagonian squid *Loligo gahi* and growth parameter estimates using least-squares fits to linear and von Bertalanffy models. Marine Ecology Progress Series 47: 65-74.

Payá, I. 2010. Fishery Report. *Loligo gahi*, Second Season 2009. Fishery statistics, biological trends, stock assessment and risk analysis. Technical Document, Falkland Islands Fisheries Dept. 54 p.

Pierce, G.J., Guerra, A. 1994. Stock assessment methods used for cephalopod fisheries. Fisheries Research 21: 255 – 285.

Piet, G.J., Hintzen, N.T. 2012. Indicators of fishing pressure and seafloor integrity. ICES Journal of Marine Science 69: 1850-1858.

Punt, A.E., Hilborn, R. 1997. Fisheries stock assessment and decision analysis: the Bayesian approach. Reviews in Fish Biology and Fisheries 7:35-63.

Roa-Ureta, R. 2012. Modelling in-season pulses of recruitment and hyperstability-hyperdepletion in the *Loligo gahi* fishery around the Falkland Islands with generalized depletion models. ICES Journal of Marine Science 69: 1403–1415.

Roa-Ureta, R., Arkhipkin, A.I. 2007. Short-term stock assessment of *Loligo gahi* at the Falkland Islands: sequential use of stochastic biomass projection and stock depletion models. ICES Journal of Marine Science 64: 3-17.

Roberts, G. 2020. Observer Report 1255. Technical Document, FIG Fisheries Department. 42 p.

Rosenberg, A.A., Kirkwood, G.P., Crombie, J.A., Beddington, J.R. 1990. The assessment of stocks of annual squid species. Fisheries Research 8: 335-350.

Shaw, P.W., Arkhipkin, A.I., Adcock, G.J., Burnett, W.J., Carvalho, G.R., Scherbich, J.N., Villegas, P.A. 2004. DNA markers indicate that distinct spawning cohorts and aggregations of Patagonian squid, *Loligo gahi*, do not represent genetically discrete subpopulations. Marine Biology, 144: 961-970.

Swartzman, G., Huang, C., Kaluzny, S. 1992. Spatial analysis of Bering Sea groundfish survey data using generalized additive models. Canadian Journal of Fisheries and Aquatic Sciences 49: 1366-1378.

Tutjavi, V. 2020. Observer Report 1251. Technical Document, FIG Fisheries Department. 25 p.

Winter, A. 2014. *Loligo* stock assessment, second season 2014. Technical Document, Falkland Islands Fisheries Department. 30 p.

Winter, A. 2015. *Loligo* stock assessment, First season 2015. Technical Document, Falkland Islands Fisheries Department. 28 p.

Winter, A. 2017. Stock assessment – *Doryteuthis gahi* 2nd season 2017. Technical Document, Falkland Islands Fisheries Department. 37 p.

Winter, A. 2018. Stock assessment – *Doryteuthis gahi* 1st season 2018. Technical Document, Falkland Islands Fisheries Department. 36 p.

Winter, A. 2019a. Stock assessment –Falkland calamari *Doryteuthis gahi* 1st season 2019. Technical Document, Falkland Islands Fisheries Department. 37 p.

Winter, A. 2019b. Stock assessment –Falkland calamari *Doryteuthis gahi* 2nd season 2019. Technical Document, Falkland Islands Fisheries Department. 36 p.

Winter, A., Arkhipkin, A. 2015. Environmental impacts on recruitment migrations of Patagonian longfin squid (*Doryteuthis gahi*) in the Falkland Islands with reference to stock assessment. Fisheries Research 172: 85-95.

Winter, A., Lee, B., Arkhipkin, A., Tutjavi, V., Büring, T. 2020. Falkland calamari (*Doryteuthis gahi*) stock assessment survey, 1st season 2020. Technical Document, Falkland Islands Fisheries Department. 16 p.

Appendix
***Doryteuthis gahi* individual weights**

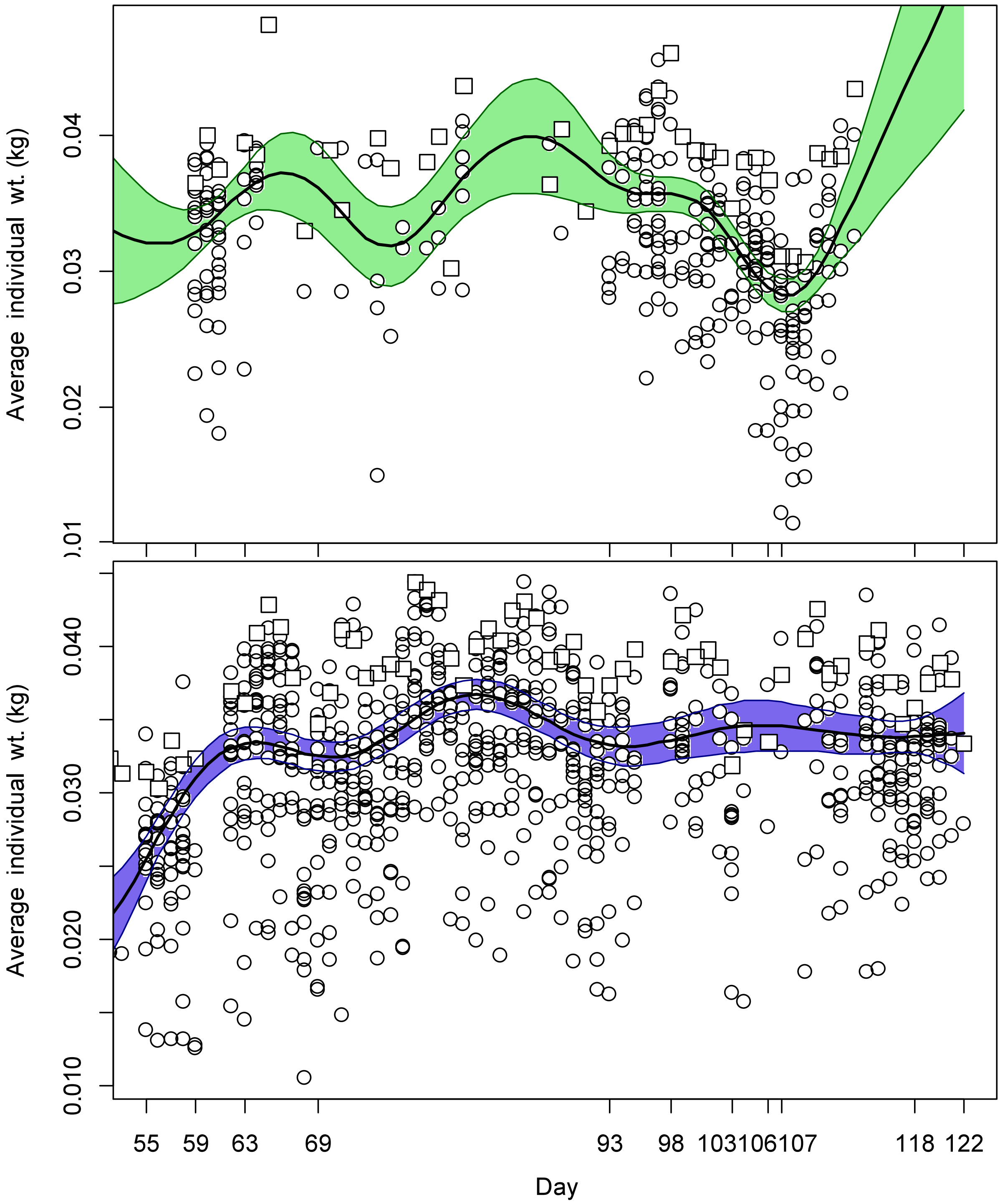

Figure A1. North (top) and south (bottom) sub-area daily average individual *D. gahi* weights from commercial size categories per vessel (circles) and observer measurements (squares). GAMs of the daily trends ± 95% confidence intervals (centre lines and colour under-shading).

To smooth fluctuations, GAM trends were calculated of daily average individual weights. North and south sub-areas were calculated separately. For continuity, GAMs were calculated using all pre-season survey and in-season data contiguously. North and south GAMs were first calculated separately on the commercial and observer data. Commercial data GAMs were taken as the baseline trends, and calibrated to observer data GAMs in proportion to the correlation between commercial data and observer data GAMs. For example, if the season average individual weight estimate from commercial data was 0.052 kg, the season average individual weight estimate from observer data was 0.060 kg, and the coefficient of determination (R^2) between commercial and observer GAM trends was 86%, then the resulting trend of daily average individual weights was calculated as the commercial data GAM values + (0.060 – 0.052) × 0.86. This way, both the greater day-to-day consistency of the commercial data trends, and the greater point value accuracy of the observer data are represented in the calculations. GAM plots of the north and south sub-areas are in Figure A1.

Prior estimates and CV

The pre-season survey had estimated *D. gahi* biomasses of 7,306 t north of 52° S and 20,685 t south of 52° S (Winter et al. 2020). Hierarchical bootstrapping of the inverse distance weighting algorithm obtained a coefficient of variation (CV) of 19.4% of the survey biomass distributions. From modelled survey catchability, Payá (2010) had estimated average net escapement of up to 22%, which was added to the CV:

$$20{,}685 \pm (.194 + .22) = 20{,}685 \pm 41.4\% \quad = 20{,}685 \pm 8{,}570 \text{ t} \qquad \textbf{(A1-S)}$$

$$7{,}306 \pm (.194 + .22) = 7{,}306 \pm 41.4\% \quad = 07{,}306 \pm 3{,}027 \text{ t} \qquad \textbf{(A1-N)}$$

The 22% escapement was added as a linear increase in the variability, but was not used to reduce the total estimate, because squid that escape one trawl are likely to be part of the biomass concentration that is available to the next trawl.

D. gahi numbers at the end of the survey were estimated as the survey biomasses divided by the GAM-predicted individual weight averages for the survey: 0.0229 kg south, 0.0361 kg north (Figure A1), 0.0230 kg combined. Average coefficients of variation (CV) of the GAM over the duration of the pre-season survey were 7.4% south, 8.5% north. CV of the length-weight conversion relationship (Equation 7) were 10.3% south, 8.4% north. Joining these sources of variation with the pre-season survey biomass estimates and individual weight averages (above) gave estimated *D. gahi* numbers at survey end (day 53) of:

$$_{\text{prior}}N_{\text{S day 53}} = \frac{20{,}685 \times 1000}{0.0229} \pm \sqrt{41.4\%^2 + 7.4\%^2 + 10.3\%^2}$$

$$= 0.903 \times 10^9 \pm 43.3\%$$

$$_{\text{prior}}N_{\text{N day 53}} = \frac{7306 \times 1000}{0.0361} \pm \sqrt{41.4\%^2 + 8.5\%^2 + 8.4\%^2}$$

$$= 0.202 \times 10^9 \pm 43.1\%$$

Priors were normalized for the combined fishing zone average, to produce better continuity as vessels cross back and forth between north and south:

$$_{\text{nprior}}N_{\text{S day 53}} = \left(\frac{(20{,}685 + 7306) \times 1000}{0.0230}\right) \times \left(\frac{_{\text{prior}}N_{\text{S day 53}}}{_{\text{prior}}N_{\text{N day 53}} + {_{\text{prior}}N_{\text{S day 53}}}}\right)$$

$$= 0.996 \times 10^{9} \pm 43.3\% \qquad \textbf{(A2-S)}$$

$$_{\text{nprior}}N_{\text{N day 53}} = \left(\frac{(20{,}685 + 7306) \times 1000}{0.0230}\right) \times \left(\frac{_{\text{prior}}N_{\text{N day 53}}}{_{\text{prior}}N_{\text{N day 53}} + {_{\text{prior}}N_{\text{S day 53}}}}\right)$$

$$= 0.223 \times 10^{9} \pm 43.1\% \qquad \textbf{(A2-N)}$$

The catchability coefficient (q) prior for the south sub-area was taken on day 55, the first day of the season, when 15 vessels fished in the south and the initial depletion period south started. Abundance on day 55 was discounted for natural mortality over the 2 days since the end of the survey:

$$_{\text{nprior}}N_{\text{S day 55}} = {_{\text{nprior}}N_{\text{S day 53}}} \times e^{-M\cdot(55-53)} - CNMD_{\text{S day 55}} = 0.970 \times 10^{9} \qquad \textbf{(A3-S)}$$

where $CNMD_{\text{S day 55}} = 0$ as no catches intervened between the end of the survey and the start of commercial season. Thus:

$$_{\text{prior}}q_{\text{S}} = C(N)_{\text{S day 55}} / ({_{\text{nprior}}N_{\text{S day 55}}} \times E_{\text{S day 55}})$$

$$= (C(B)_{\text{S day 55}} / Wt_{\text{S day 55}}) / ({_{\text{nprior}}N_{\text{S day 55}}} \times E_{\text{S day 55}})$$

$$= (652.6\text{ t} / 0.025513\text{ kg}) / (0.970 \times 10^{9} \times 15\text{ vessel-days})$$

$$= 1.758 \times 10^{-3}\ \text{vessels}^{-1} \qquad \textbf{(A4-S)}$$ [g]

CV of the prior was calculated as the sum of variability in $_{\text{nprior}}N_{\text{S day 53}}$ (Equation **A2-S**) plus variability in the catches of vessels on start day 55, plus variability of the natural mortality (see Appendix section Natural mortality, below):

$$CV_{\text{prior S}} =$$

$$\sqrt{43.3\%^2 + \left(\frac{\text{SD}\left(C(B)_{\text{S vessels day 55}}\right)}{\text{mean}\left(C(B)_{\text{S vessels day 55}}\right)}\right)^2 + \left(1 - \text{sign}(1 - CV_M) \times \text{abs}(1 - CV_M)^{(55-53)}\right)^2}$$

$$= \sqrt{43.3\%^2 + 32.1\%^2 + 28.5\%^2} = 61.0\% \qquad \textbf{(A5-S)}$$

The catchability coefficient (q) prior for the north sub-area was taken on day 59, the first day that fishing was undertaken in the north by 12 vessels (Figure 4) and the initial depletion period north started. Abundance on day 59 was discounted for natural mortality over the 6 days since the end of the survey:

$$_{\text{nprior}}N_{\text{N day 55}} = {_{\text{nprior}}N_{\text{N day 53}}} \times e^{-M\cdot(59-53)} - CNMD_{\text{N day 59}} = 0.206 \times 10^{9} \qquad \textbf{(A3-N)}$$

where $CNMD_{\text{N day 59}} = 0$ as in the north also no catches intervened between the end of the survey and the start of commercial season. Thus:

[g] On Figure 7-left.

$$
\begin{aligned}
{}_{\text{prior}}q_{\text{N}} &= C(N)_{\text{N day 59}} / ({}_{\text{nprior}}N_{\text{N day 59}} \times E_{\text{N day 59}}) \\
&= (C(B)_{\text{N day 59}} / Wt_{\text{N day 59}}) / ({}_{\text{nprior}}N_{\text{N day 59}} \times E_{\text{N day 59}}) \\
&= (664.2\ \text{t} / 0.032778\ \text{kg}) / (0.206 \times 10^{9} \times 12\ \text{vessel-days}) \\
&= 8.206 \times 10^{-3}\ \text{vessels}^{-1}\ {}^{\text{h}}
\end{aligned}
\qquad \textbf{(A4-N)}
$$

CV of the prior was calculated as the sum of variability in ${}_{\text{nprior}}N_{\text{N day 53}}$ (Equation **A2-N**) plus variability in the catches of vessels on start day 59, plus variability of the natural mortality (see Appendix section Natural mortality, below):

$$
CV_{\text{prior N}} =
$$

$$
\sqrt{43.1\%^2 + \left(\frac{\mathrm{SD}\left(C(B)_{\text{N vessels day 59}}\right)}{\mathrm{mean}\left(C(B)_{\text{N vessels day 59}}\right)}\right)^2 + (1 - \mathrm{sign}(1 - CV_M) \times \mathrm{abs}(1 - CV_M)^{(59-53)})^2}
$$

$$
= \sqrt{43.1\%^2 + 24.4\%^2 + 63.5\%^2} \quad = 80.5\% \qquad \textbf{(A5-N)}
$$

Depletion model estimates and CV

For the south sub-area, the equivalent of Equation **2** with six N_{day} was optimized on the difference between predicted and actual catches (Equation **3**), resulting in parameters values:

$$
\begin{aligned}
{}_{\text{depletion}}N1_{\text{S day 55}} &= 1.206 \times 10^{9}; & {}_{\text{depletion}}N2_{\text{S day 63}} &= 0.064 \times 10^{6} \\
{}_{\text{depletion}}N3_{\text{S day 69}} &= 0.046 \times 10^{6}; & {}_{\text{depletion}}N4_{\text{S day 98}} &= 0.174 \times 10^{9} \\
{}_{\text{depletion}}N5_{\text{S day 106}} &= 0.099 \times 10^{9}; & {}_{\text{depletion}}N6_{\text{S day 118}} &= 0.319 \times 10^{9} \\
{}_{\text{depletion}}q_{\text{S}} &= 1.390 \times 10^{-3}\ {}^{\text{i}}
\end{aligned}
\qquad \textbf{(A6-S)}
$$

The normalized root-mean-square deviation of predicted vs. actual catches was calculated as the CV of the model:

$$
CV_{\text{rmsd S}} = \frac{\sqrt{\sum_{i=1}^{n}\left({}_{\text{predicted}}C(N)_{\text{S day i}} - {}_{\text{actual}}C(N)_{\text{S day i}}\right)^2 / n}}{\mathrm{mean}\left({}_{\text{actual}}C(N)_{\text{S day i}}\right)}
$$

$$
= 2.063 \times 10^{6} / 9.694 \times 10^{6} = 21.3\% \qquad \textbf{(A7-S)}
$$

$CV_{\text{rmsd S}}$ was added to the variability of the GAM-predicted individual weight averages for the season (Figure A1-S); equal to a CV of 1.9% south. CVs of the depletion were then calculated as the sum:

$$
CV_{\text{depletion S}} = \sqrt{CV_{\text{rmsd S}}^{\ 2} + CV_{\text{GAM Wt S}}^{\ 2}} = \sqrt{21.3\%^2 + 1.9\%^2}
$$

[h] On Figure 9-left.
[i] On Figure 7-left.

$$= \quad 21.4\% \qquad \textbf{(A8-S)}$$

For the north sub-area, the Equation **2** equivalent with five N $_{day}$ was optimized on the difference between predicted and actual catches (Equation **3**), resulting in parameter values:

$${}_{depletion}N1_{N\ day\ 59} = 0.009 \times 10^9; \qquad {}_{depletion}N2_{N\ day\ 63} = 0.001 \times 10^6$$
$${}_{depletion}N3_{N\ day\ 93} = 0.069 \times 10^9; \qquad {}_{depletion}N4_{N\ day\ 103} = 0.038 \times 10^9$$
$${}_{depletion}N5_{N\ day\ 107} = 0.063 \times 10^9$$
$${}_{depletion}q_{N} = 1.879 \times 10^{-2} \text{ [j]} \qquad \textbf{(A6-N)}$$

Root-mean-square deviation of predicted vs. actual catches was calculated as the CV of the model:

$$CV_{rmsd\ N} = \frac{\sqrt{\sum_{i=1}^{n}\left({}_{predicted}C(N)_{N\ day\ i} - {}_{actual}C(N)_{N\ day\ i}\right)^2 / n}}{\text{mean}\left({}_{actual}C(N)_{N\ day\ i}\right)}$$

$$= 2.183 \times 10^6 / 3.503 \times 10^6 = 62.3\% \qquad \textbf{(A7-N)}$$

$CV_{rmsd\ N}$ was added to the variability of the GAM-predicted individual weight averages for the season (Figure A1-N); equal to a CV of 2.9% north. CVs of the depletion were then calculated as the sum:

$$CV_{depletion\ N} = \sqrt{CV_{rmsd\ N}^{\ 2} + CV_{GAM\ Wt\ N}^{\ 2}} = \sqrt{62.3\%^2 + 2.9\%^2}$$

$$= \quad 62.4\% \qquad \textbf{(A8-N)}$$

Combined Bayesian models

For the south sub-area, joint optimization of Equations **3** and **4** resulted in parameters values:

$${}_{Bayesian}N1_{S\ day\ 55} = 1.064 \times 10^9; \qquad {}_{Bayesian}N2_{S\ day\ 63} = 0.042 \times 10^9$$
$${}_{Bayesian}N3_{S\ day\ 69} = 0.014 \times 10^9; \qquad {}_{Bayesian}N4_{S\ day\ 98} = 0.166 \times 10^9$$
$${}_{Bayesian}N3_{S\ day\ 106} = 0.092 \times 10^9; \qquad {}_{Bayesian}N4_{S\ day\ 118} = 0.291 \times 10^9$$
$${}_{Bayesian}q_{S} = 1.565 \times 10^{-3} \text{ [k]} \qquad \textbf{(A9-S)}$$

For the north sub-area, joint optimization of Equations **3** and **4** resulted in parameters values:

$${}_{Bayesian}N1_{N\ day\ 59} = 0.114 \times 10^9; \qquad {}_{Bayesian}N2_{N\ day\ 63} = 0.002 \times 10^6$$
$${}_{Bayesian}N3_{N\ day\ 93} = 0.093 \times 10^9; \qquad {}_{Bayesian}N4_{N\ day\ 103} = 0.047 \times 10^9$$
$${}_{Bayesian}N3_{N\ day\ 107} = 0.058 \times 10^9$$
$${}_{Bayesian}q_{N} = 8.789 \times 10^{-3} \text{ [l]} \qquad \textbf{(A9-N)}$$

These parameters produced the fit between predicted catches and actual catches shown in Figures A2-S and A2-N.

[j] Off the scale on Figure 9-left.
[k] On Figure 7-left.
[l] On Figure 9-left.

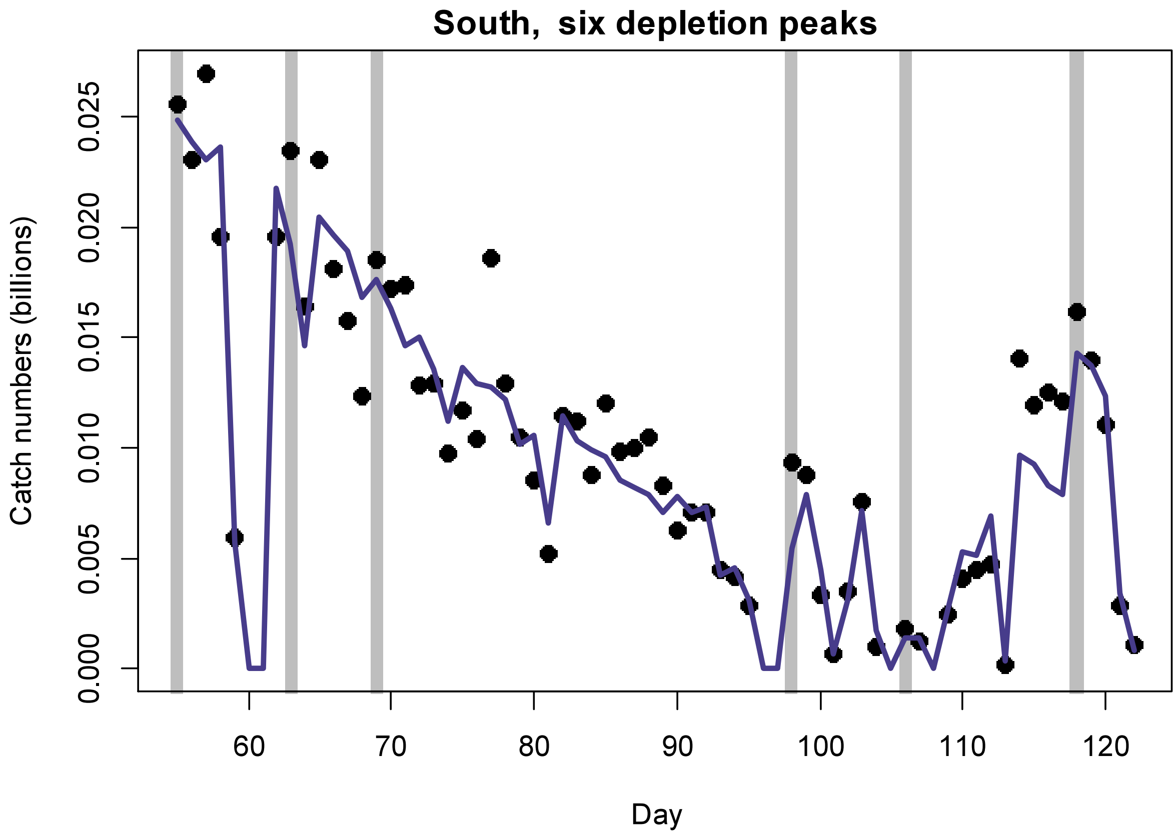
South, six depletion peaks
Catch numbers (billions)
0.000
0.005
0.010
0.015
0.020
0.025
60
70
80
90
100
110
120
Day

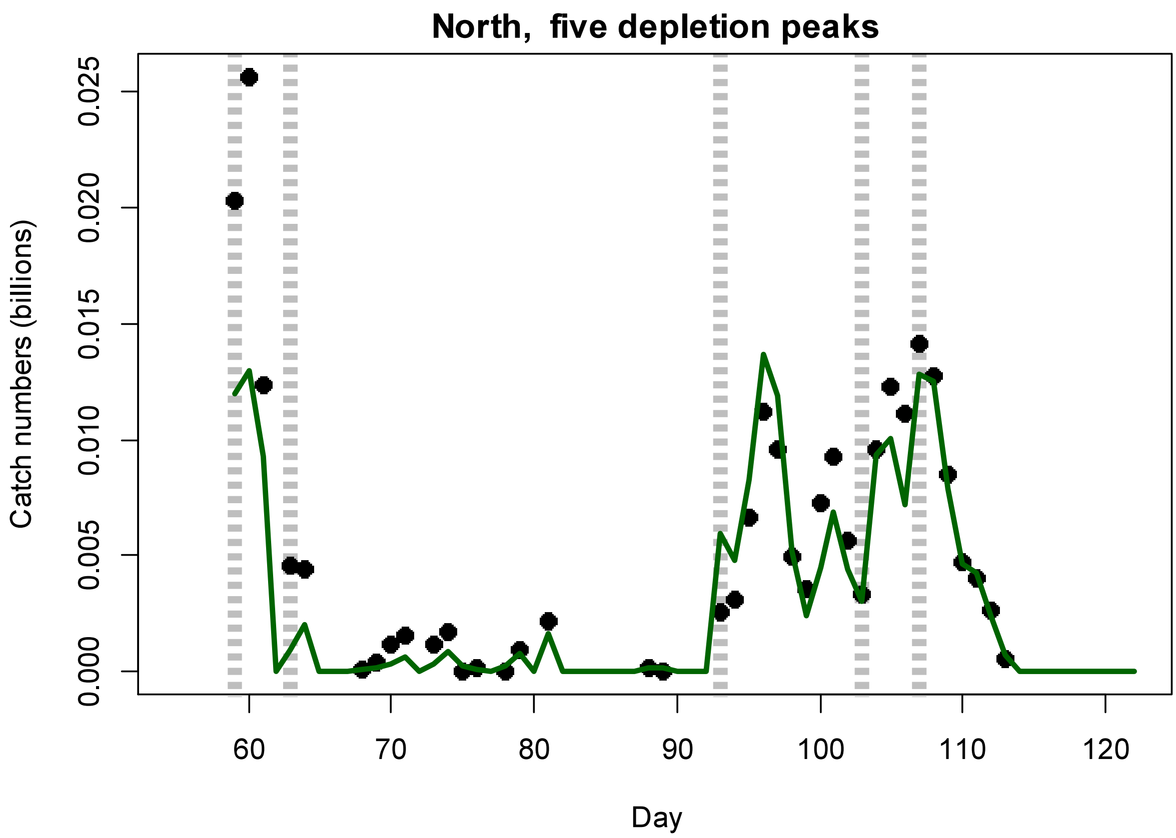
North, five depletion peaks
Catch numbers (billions)
0.000
0.005
0.010
0.015
0.020
0.025
60
70
80
90
100
110
120
Day

Figure A2-S [previous page top]. Daily catch numbers estimated from actual catch (black points) and predicted from the depletion model (purple line) in the south sub-area.

Figure A2-N [previous page bottom]. Daily catch numbers estimated from actual catch (black points) and predicted from the depletion model (green line) in the north sub-area.

Natural mortality

Natural mortality is parameterized as a constant instantaneous rate M = 0.0133 day^{-1} (Roa-Ureta and Arkhipkin 2007), based on Hoenig's (1983) log mortality vs. log maximum age regression applied to an estimated maximum age of 352 days for *D. gahi*:

$$\log(M) = 1.44 - 0.982 \times \log(\text{age}_{max})$$

$$M = \exp(1.44 - 0.982 \times \log(352))$$

$$= 0.0133 \qquad \textbf{(A10)}$$

Hoenig (1983) derived Equation **A10** from the regression of 134 stocks among 79 species of fish, molluscs, and cetaceans. Hoenig's regression obtained $R^2 = 0.82$, but a corresponding coefficient of variation (CV) was not published. An approximate CV of M was estimated by measuring the coordinates off a print of Figure 1 in Hoenig (1983) and repeating the regression. Variability of M was calculated by randomly re-sampling, with replacement, the regression coordinates 10000× and re-computing Equation **A10** for each iteration of the resample. The CV of M from the 10000 random resamples was:

$$CV_M = SD_M / Mean_M$$

$$CV_M = 0.0021 / 0.0134 = 15.46\% \qquad \textbf{(A11)}$$

CV_M over the aggregate number of unassessed days between survey end and commercial season start was then added to the CV of the biomass prior estimate and the CV of variability in vessel catches on start day (Equations **A5-S** and **A5-N**). CV_M was further expressed as an absolute value and indexed by sign(1 - CV_M) to ensure that the value could not decrease if CV_M was hypothetically > 100%.

Total catch by species

Table A1: Total reported catches and discard by taxon during 1st season 2020 C-license fishing, and number of catch reports in which each taxon occurred. Does not include incidental catches of pinnipeds or seabirds.

Species Code	Species / Taxon	Catch Wt. (KG)	Discard Wt. (KG)	N Reports
LOL	*Doryteuthis gahi*	29116101	18115	1012
PAR	*Patagonotothen ramsayi*	261734	261724	956
HAK	*Merluccius hubbsi*	117461	8387	404
WHI	*Macruronus magellanicus*	87633	10166	165
MUN	*Munida* spp.	10889	10889	67

CGO	*Cottoperca gobio*	10129	10115	595
RAY	Rajiformes	9894	6461	505
BUT	*Stromateus brasiliensis*	6527	6366	262
ILL	*Illex argentinus*	5025	1080	237
PTE	*Patagonotothen tessellata*	3862	3871	73
SCA	Scallop	3531	3531	176
UCH	Sea urchin	1930	1930	87
BAC	*Salilota australis*	1901	799	142
TOO	*Dissostichus eleginoides*	1768	1701	267
GRV	*Macrourus* spp.	1522	1085	72
ING	*Moroteuthis ingens*	1486	1483	193
KIN	*Genypterus blacodes*	1478	1445	228
DGH	*Schroederichthys bivius*	1401	1397	209
ALF	*Allothunnus fallai*	1017	1017	92
OCT	*Octopus* spp.	960	960	112
GRC	*Macrourus carinatus*	789	33	4
POR	*Lamna nasus*	281	281	3
GRF	*Coelorhynchus fasciatus*	190	190	3
DGS	*Squalus acanthias*	156	156	27
SEP	*Seriolella porosa*	81	81	12
CHE	*Champsocephalus esox*	60	60	11
SAR	*Sprattus fuegensis*	50	50	5
BLU	*Micromesistius australis*	50	50	3
SPN	Porifera	32	32	4
MED	Medusae sp.	28	28	4
COP	*Congiopodus peruvianus*	24	24	5
PAT	*Merluccius australis*	21	21	8
GRX	*Coelorhynchus* sp. Cf *braueri*	20	20	1
RED	*Sebastes oculatus*	6	6	2
MYX	*Myxine* spp.	5	5	3
PRO	*Procellaria aequinoctialis*	2	2	2
EEL	*Iluocoetes fimbriatus*	1	1	1
DGX	Dogfish / Catshark	1	1	1
SOM	*Somniosus microcephalus*	0	0	1
Total		29648046	353563	1012